

Photochemical behavior of (diphosphine)(η^2 -tolane)Pt⁰ complexes. Part A: Experimental considerations in solution and in the solid state†

Thomas Weisheit,^a Daniel Escudero,^b Holm Petzold,^c Helmar Görls,^a Leticia González^b and Wolfgang Weigand^{*a}

Received 9th December 2009, Accepted 13th August 2010

DOI: 10.1039/b925562a

A series of various (diphosphine)(η^2 -tolane)Pt⁰ complexes exhibiting manifold substitution pattern of the tolane ligand (**5a–g**) and different rigid diphosphines defining various bite angles at the Pt center (**9a–b**) have been synthesized. All compounds were isolated and characterized by means of spectroscopic methods and additionally by X-ray structure determination (**5a–e**, **9a–b**). In view of potential C_{aryl}–C_{ethynyl} bond activation, we investigated their photochemical behavior in the solid state as well as in solution by irradiating with sunlight. The reactivity towards C_{aryl}–C_{ethynyl} bond activation in the crystalline state and in solution is discussed in relation to substituents attached to the tolane ligand and on the extent of the torsion of its phenyl rings. Complexes **5a–c** and **9a** either bearing electron withdrawing bromides or possessing a large dihedral angle of the phenyl rings, showed selective oxidative addition of the C_{aryl}–C_{ethynyl} bond to the Pt center in the solid state, yielding complexes **6a–c** and **10a**, respectively. In contrast, **5d–f** and **9b** proved to be unreactive under similar conditions because of their electron donating methoxy groups as well as the reduced twisting of their phenyl or pyridyl moieties of the tolane ligands. Irradiation of complexes **5a** and **5b** with sunlight in solution revealed the formation of the appropriate C–Br activated compounds **7a** and **7b** along with **6a** and **6b** in a 1 : 1 mixture. The observed photochemical C_{aryl}–C_{ethynyl} bond activation is reversible under thermal conditions, regaining the appropriate Pt⁰ complexes by reductive elimination.

Introduction

The activation of carbon–carbon bonds by using metal complexes in a homogeneous medium has attracted much interest particular in view of applications in petroleum chemistry.^{1–3} During the last decades some examples for C–C bond activation by means of oxidative addition on a metal complex have been reported. Most of them are driven by relief of ring strain^{2–4} in the corresponding insertion products or the fact that the C–C bond is forced to react with the metal center by proximity.^{3,5,6} On the other hand, only a few examples for the activation of unstrained C–C bonds are known so far.^{6,7} The principal reasons for this scarcity of examples might be the more favorable C–H bond activation due to the higher activation barrier of C–C bonds⁸ and the considerably increased stability of the resulting metal–hydrogen bond in comparison with the corresponding metal–carbon bond.⁹ However, C–C bond cleavage also depends on the nature of the respective C–C bond. Although C_{aryl}–C_{aryl} or C_{aryl}–C_{alkyl} bonds are generally stronger than C_{alkyl}–C_{alkyl} bonds their activation by rhodium or iridium complexes

has been reported.^{9,10} The determined metal–C_{aryl} bond strength of the resulting product, which is significantly higher than that of a metal–C_{alkyl} bond, was supposed to be the driving force of these reactions.

However, beside the thermal activation of inactivated C–C bonds, Jones *et al.* reported on the oxidative addition of Pt⁰ complex fragments to the C_{aryl}–C_{ethynyl} bond of coordinated diphenylacetylene derivatives (tolanes) *via* irradiating solutions of these complexes with UV light.^{11,12} Interestingly, C–C bond cleavage in this system is only observed under photochemical conditions and not *via* thermal treatment of the Pt⁰ complexes.

Therefore, the framework of a tolane ligand coordinated to a (diphosphine)Pt⁰ complex fragment is estimated to be an efficient system for studying the driving force of this type of photochemical C–C bond activation. In this context, Jones *et al.* investigated the influence of the substitution pattern of the tolane ligand on the photochemical reactivity of its appropriate platinum complex.¹² It was shown that stabilization of the addition products is achieved when electron withdrawing groups were introduced and therefore, the activation energy of the bond cleavage can be tuned by the choice of the acetylenic ligand.

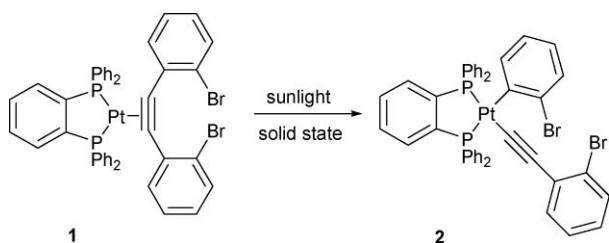
Recently we could show that the aforementioned C–C bond activation is not restricted to the solution state. By irradiating crystals of (dppbe)(η^2 -2,2'-dibromotolane)Pt⁰ (**1**) with sunlight a highly selective insertion of the (dppbe)Pt moiety into the C_{aryl}–C_{ethynyl} bond was observed (Scheme 1).¹³ The different photochemistry of this complex compared to that of (dppbe)(η^2 -tolane)Pt⁰ was explained by remarkable differences in their calculated UV/Vis spectra and electronic transitions included therein.¹³ A conspicuous feature of **1** in the solid state is the twisting of

^aInstitut für Anorganische und Analytische Chemie, Friedrich-Schiller-Universität Jena, August-Bebel-Str. 2, 07743, Jena, Germany. E-mail: wolfgang.weigand@uni-jena.de; Fax: +49-3641-948102; Tel: +49-3641-948160

^bInstitut für Physikalische Chemie, Friedrich-Schiller-Universität Jena, Helmholzweg 4, 807743, Jena, Germany

^cTU Chemnitz, Institut für Chemie, Straße der Nationen 62, 09111, Chemnitz, Germany

† CCDC reference numbers 743160 (for **5a**), 743161 (for **5b**), 743162 (for **5c**), 743163 (for **5d**), 743164 (for **5e**), 743165 (for **6b**), 743166 (for **7b**), 743167 (for **9a**) and 743269 (for **9b**). For crystallographic data in CIF or other electronic format see DOI: 10.1039/b925562a



Scheme 1 Selective C–C bond cleavage in the solid state *via* irradiation of crystals of (dppbe)(η^2 -2,2'-dibromotolane)Pt⁰ with sunlight.

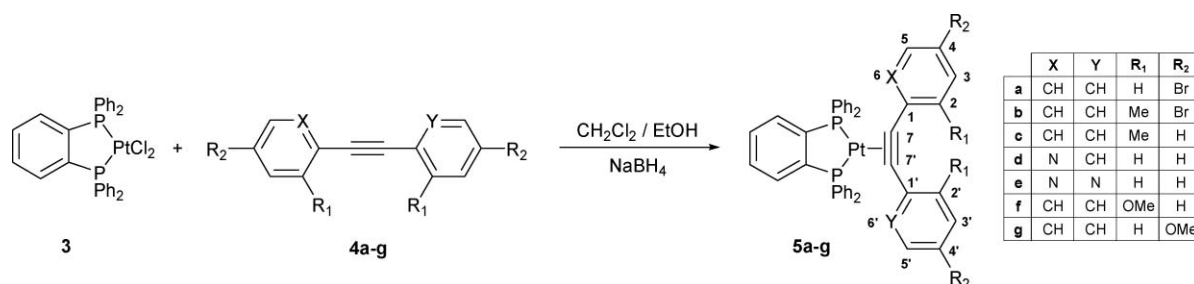
either phenyl groups of the tolane ligand against each other. Their spatial orientation is caused by the repulsion of both *ortho*-bonded bromine atoms.¹³ Additionally, the reported solid-state reaction of **1** might be explained by the electron-withdrawing nature of the bromine atoms as well.

In order to study the effect of the spatial orientation of the phenyl groups as well as the influence of attached electron donating groups (EDGs) and electron withdrawing groups (EWGs), we synthesized a series of novel (diphosphine)Pt⁰ complexes with different tolane ligands. Hence, their photochemical behavior in the solid state as well as in solution was paid main attention to. A detailed discussion supported by density functional theory (DFT) and time-dependent density functional theory (TD-DFT) methods of the different reactivity will be given in part B.‡

Results and discussion

According to our previously reported synthesis of (diphosphine)(nbe)Pt⁰ [nbe = norbornene] complexes,¹⁴ the required (dppbe)Pt(η^2 -tolane) complexes **5a–g** were prepared by reaction of (dppbe)PtCl₂ (**3**) with sodium borohydride in dichloromethane–ethanol and subsequent treatment with the appropriate tolane derivative **4a–g** (Scheme 2). Complexes **5a–g** were obtained analytically pure as yellow to orange solids *via* crystallization by diffusion of pentane into concentrated toluene or benzene solutions of the appropriate crude products. The ³¹P{¹H} NMR spectra of **5a–c** and **5e–g** revealed a singlet along with the appropriate ¹⁹⁵Pt satellites, pointing to their symmetrical conformation. In contrast, the unsymmetrical complex **5d** shows an AB spin-system pattern in the ³¹P{¹H} NMR spectrum, consisting of two coinciding doublets together with ¹⁹⁵Pt satellites.

‡ D. Escudero, T. Weisheit, W. Weigand and L. González, Photochemical behavior of (diphosphine)(η^2 -tolane)Pt⁰ complexes in solution and in the solid state; Part B: Theoretical part, *Dalton Trans.*, 2010, **39**, DOI: 10.1039/B925928G.



Scheme 2 Synthesis of (dppbe)(η^2 -tolane)Pt⁰ complexes **5a–g**.

The chemical shifts (51.3–52.6 ppm) as well as the ¹J_{Pt} coupling constants (3063–3143 Hz) of **5a–g** are in a narrow range, suggesting only minor influence of the acetylene ligand on the electronic nature of the Pt complex fragment. The purity and constitution of **5a–g** were confirmed by satisfying elemental analysis as well as mass spectrometry. Additionally, the results of the X-ray structure determination of **5a–e** (Fig. 1) prove the proposed structures of these complexes. Selected bond lengths and angles are summarized in Table 1 and are comparable with those reported for related Pt⁰-tolane complexes.^{11–15} The experimentally measured values are in good agreement with the theoretically calculated ones (Table 1). Noteworthy differences are only observed for torsion angles C(8)–C(3)–C(9)–C(14), which are more sensitive to packing effects. The arrangement of the ligands around the platinum center is distorted square-planar for each complex. Due to the π back donation ($d_{Pt} \rightarrow \pi^*_{alkyne}$) the bond lengths C(1)–C(2) are significantly longer than those reported for uncoordinated alkynes.¹⁶ Furthermore, the decline of the angles C(1)–C(2)–C(3) and C(2)–C(1)–C(9), compared to uncoordinated tolanes (180°), is in good accordance with the increased alkene character of the formerly alkynes. The importance of the π back donation in these complexes was also verified by means of natural-bond-order (NBO) calculations.¹⁷

As a consequence of the π back donation, the wave numbers of the $\nu(C\equiv C)$ are conspicuously shifted to smaller values for coordinated alkynes.¹⁶

In continuation of the results achieved with **1**, we first focused on the photoreactions of **5a** in the solid state and in solution. This complex shows a torsion angle C(8)–C(3)–C(9)–C(14) (see Table 1) of 30.7°, which is remarkably smaller than that of **1**, promising decreased steric influence compared to **1**. Nevertheless, both bromine atoms in *para*-position should provide a comparable electronic contribution to the reactivity as observed for **1**. Indeed, the irradiation of crystalline **5a** with sunlight for 12 days resulted in the selective conversion into a new unsymmetrical complex in 90% yield based on the ³¹P{¹H} NMR data. Its ³¹P{¹H} NMR spectrum shows two doublets at 50.6 and 49.2 ppm along with ¹⁹⁵Pt satellites. The observed ¹J_{Pt} coupling constants (2467/1575 Hz) agree with the formation of the corresponding C–C activated counterpart **6a** (Scheme 3). Complex **6a** was isolated by column chromatography and obtained as pale yellow powder. Strong absorption at $\nu = 2112\text{ cm}^{-1}$ in the IR spectrum verifies the end-on coordination of the alkyne ligand. The constitution and purity of **6a** was unambiguously confirmed by mass spectrometry as well as elemental analysis.

As expected, this selectivity vanishes when **5a** is irradiated in toluene solution. The ³¹P{¹H} NMR spectrum of the reaction mixture shows two AB spin systems with corresponding ¹⁹⁵Pt

Table 1 Selected bond lengths [\AA] and angles [$^\circ$] of complexes **5a–e** and **9a–b**. The corresponding calculated values are given in italics^a

	5a	5b	5c	5d	5e	9a	9b
P(1)–Pt	2.2569(14)	2.2499(11)	2.2498(14)	2.2650(13)	2.2508(14)	2.2541(14)	2.2658(14)
	2.333	2.333	2.324	2.335	2.333	2.319	2.344
P(2)–Pt	2.2583(14)	2.2463(11)	2.2686(13)	2.2566(13)	2.2453(14)	2.2507(14)	2.2707(16)
	2.335	2.325	2.331	2.333	2.328	2.315	2.348
C(1)–Pt	2.027(6)	2.049(4)	2.064(6)	2.030(5)	2.041(5)	2.047(6)	2.045(6)
	2.082	2.101	2.101	2.077	2.064	2.099	2.101
C(2)–Pt	2.039(6)	2.040(4)	2.042(5)	2.041(5)	2.027(6)	2.052(6)	2.059(6)
	2.084	2.089	2.090	2.081	2.079	2.102	2.103
C(1)–C(2)	1.295(8)	1.302(6)	1.300(7)	1.293(8)	1.299(9)	1.288(8)	1.295(8)
	1.312	1.305	1.304	1.312	1.314	1.305	1.306
P(1)–Pt–P(2)	85.00(5)	86.47(4)	86.25(5)	86.63(5)	87.28(5)	88.10(5)	102.79(5)
	85.0	85.7	85.7	84.8	85.3	91.8	102.1
C(1)–Pt–C(2)	37.1(2)	37.13(18)	36.9(2)	37.0(2)	37.3(2)	36.6(2)	36.8(2)
	36.7	36.3	36.3	36.8	37.0	36.2	36.2
C(1)–C(2)–C(3)	144.4(6)	153.2(4)	146.9(6)	144.3(5)	144.0(6)	149.1(6)	145.5(6)
	146.7	149.8	150.1	145.1	144.4	145.5	145.9
C(2)–C(1)–C(9)	145.9(6)	149.0(4)	141.2(5)	143.4(5)	144.6(6)	149.2(6)	146.8(6)
	147.5	146.6	146.9	144.7	144.9	148.4	146.0
C(8)–C(3)–C(9)–C(14) ^b	30.7(6)	63.4(4)	71.0(6)	6.4(7)	26.9(6)	121.9(6)	75.6(6)
	18.9	92.2	91.9	3.6	7.3	96.5	72.5

^a Theoretical values were calculated using the BP86/TZVP(ecp-mwb-60 for Pt) level. ^b Torsion angle between both phenyl groups of the appropriate tolane ligand; for **5d** this angle is defined as N(1)–C(3)–C(9)–C(10) and for **5e** C(4)–C(3)–C(9)–N(2), respectively.

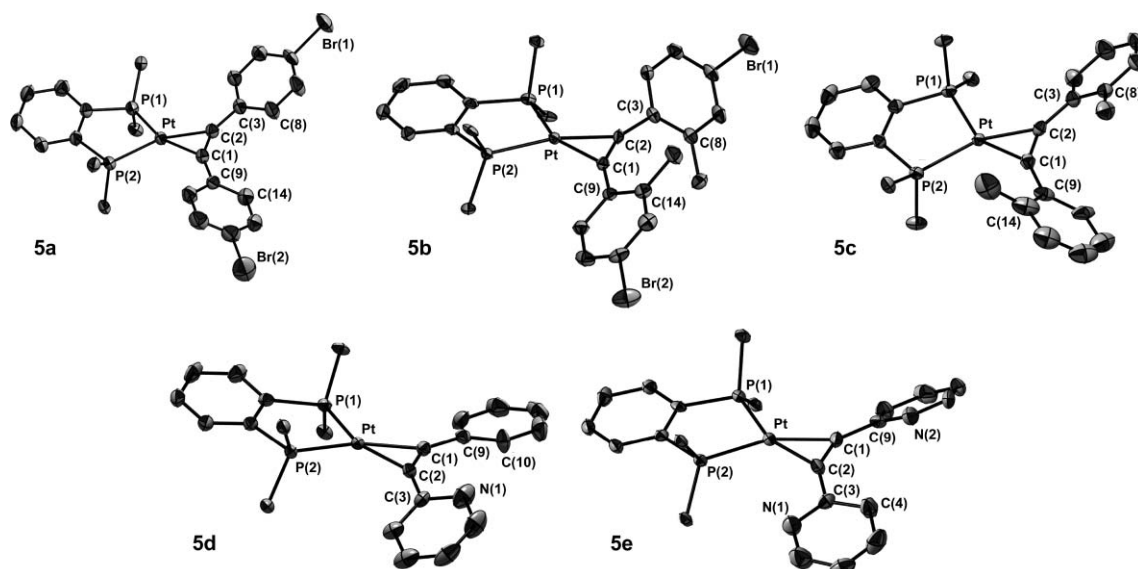
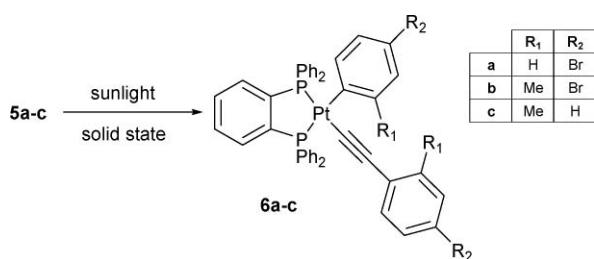


Fig. 1 Molecular structures of complexes **5a–e** with thermal ellipsoids at 50% probability level. Hydrogen atoms and solvent molecules have been omitted for clarity. The phenyl groups of the dppbe ligand are represented by their *ipso*-carbon atoms. Selected bond lengths and angles are summarized in Table 1.

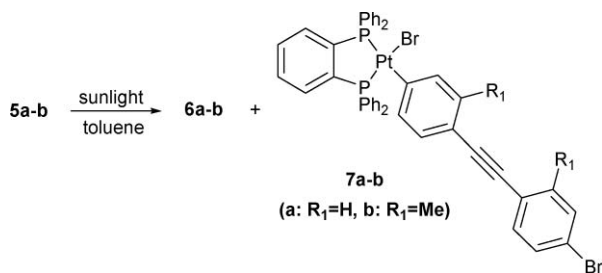
satellites, indicating the presence of two unsymmetrical complexes in a 1:1 ratio, whereas one of them was identified as **6a** and the second complex showed resonances at 49.3 and 43.2 ppm with appropriate $^1J_{\text{P,Pt}}$ coupling constants of 1658 and 3988 Hz, respectively. The value of almost 4000 Hz points to the presence of a bromine ligand *trans* to a phosphorous atom, as observed for the C–Br activated counterpart of **1**,¹³ hence the formation of complex **7a** is likely (Scheme 4), but nevertheless attempts to isolate **7a** by column chromatography failed.

These results show that the presence of the bromine moieties at the coordinated tolane ligand mainly increases the reactivity towards C–C bond activation. Indeed, the $^{31}\text{P}\{^1\text{H}\}$ NMR spectra

of irradiated samples of **5b** and **5c** revealed the conversion of the starting materials to the appropriate C–C activated Pt^{II} counterparts **6b** and **6c** (Scheme 3), indicated by two doublets along with ^{195}Pt satellites, respectively (for **6b**: 50.1/48.9 ppm, $^1J_{\text{P,Pt}} = 2474/1639$ Hz and for **6c**: 50.5/48.6 ppm, $^1J_{\text{P,Pt}} = 2469/1561$ Hz). Interestingly, after similar reaction periods 45% of **5b** are converted to **6b**, but only 25% of **5c** have been reacted to **6c**. The torsion angles of **5b** and **5c** have approximately the same value due to the *ortho*-bonded methyl groups, which should provide a comparable steric contribution to the reactivity. However, methyl groups also possess a marginal electron donating character, countervailing the electron withdrawing properties of the bromine substituents in



Scheme 3 Selective formation of the C–C activated compounds **6a–c** by irradiation of the appropriate (dppbe)(η^2 -tolane)Pt⁰ complexes with sunlight.



Scheme 4 Irradiation of the bromo-substituted complexes in solution results in the formation of the C–C activated compounds **6** and the C–Br activated ones **7** in a 1 : 1 ratio.

5b, which might explain the reduced conversion of **5b** and **5c** in comparison to **5a**.

The reaction of **5b** in toluene solution resulted in the formation of two complexes in a 1 : 1 ratio, which were found to be the C–C activated product **6b** and the C–Br activated compound **7b**, with respect to the ³¹P{¹H} NMR data of the crude product (Scheme 4). Column chromatography of the product mixture yielded both complexes in analytical purity, which was verified by spectroscopic methods and elemental analysis. The ³¹P{¹H} NMR spectra of **6b** and **7b** revealed two doublets as well as the corresponding ¹⁹⁵Pt satellites due to their unsymmetrical conformation (for **7b**: 49.6/43.0 ppm, ¹J_{P,Pt} = 1684/4090 Hz). The ¹J_{P,Pt} values of **7b** are comparable to that of **7a**, verifying the insertion of the (dppbe)Pt⁰ complex fragment into one of the C–Br bonds. The proposed molecular structures of **6b** and **7b** are unambiguously confirmed by the results of the X-ray structure determination (Fig. 2 and 3).

The arrangement of the ligands around the metal center is slightly distorted from square planarity. The remarkably enlarged bond length Pt–P(1) in comparison to Pt–P(2) in complex **7b** can be plausibly explained by the greater extent of the *trans*-influence of the sp² hybridized carbon atom. In contrast to the appropriate (dppbe)(η^2 -tolane)Pt⁰ complex, the bond lengths C(1)–C(2) and C(8)–C(9) in compounds **6b** and **7b**, respectively, are in the typical range of carbon–carbon triple bonds. Furthermore, the end-on coordination of the alkyne to the platinum atom in **6b** is underlined by the detected strong absorption at $\nu = 2110\text{ cm}^{-1}$ in the corresponding IR spectrum.

Irradiation of a toluene solution of **5c** with sunlight for approximately 10 days, results in the selective formation of **6c**. No evidence for activation of the carbon–methyl bond was detected in the ¹H and the ³¹P{¹H} NMR spectra. The yield, calculated on the basis of the ³¹P{¹H} NMR spectrum, increases to approximately

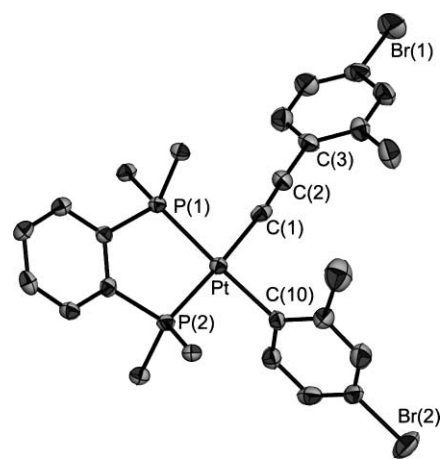


Fig. 2 Molecular structure of **6b** with thermal ellipsoids at 50% probability level. Hydrogen atoms have been omitted for clarity. The phenyl groups of the dppbe ligand are represented by their *ipso*-carbon atoms. Selected bond lengths [Å] and angles [°]: P(1)–Pt 2.2761(14), P(2)–Pt 2.2709(14), C(1)–Pt 2.022(6), C(10)–Pt 2.093(5), C(1)–C(2) 1.193(8), P(1)–Pt–P(2) 86.64(5), P(1)–Pt–C(1) 90.63(15), P(2)–Pt–C(10) 94.23(15), C(1)–Pt–C(10) 88.6(2), Pt–C(1)–C(2) 173.5(5).

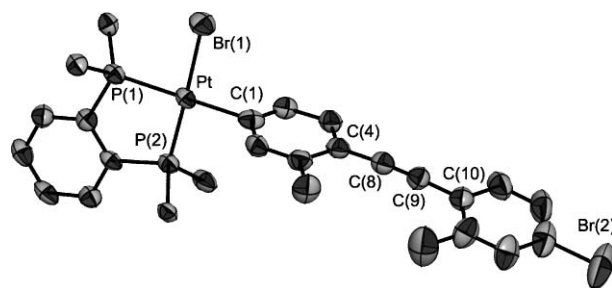


Fig. 3 Molecular structure of **7b** with thermal ellipsoids at 50% probability level. Hydrogen atoms and solvent molecules have been omitted for clarity. The phenyl groups of the dppbe ligand are represented by their *ipso*-carbon atoms. Selected bond lengths [Å] and angles [°]: P(1)–Pt 2.2806(19), P(2)–Pt 2.2082(17), C(1)–Pt 2.099(8), Pt–Br(1) 2.4679(8), C(8)–C(9) 1.176(10), P(1)–Pt–P(2) 87.62(6), P(1)–Pt–Br(1) 90.35(5), P(2)–Pt–C(1) 93.02(19), C(1)–Pt–Br(1) 89.01(18), C(4)–C(8)–C(9) 175.9(8).

75% compared with 25% in the respective experiment in the solid state.

Considering these previous observations, the question arises whether the insertion of the Pt⁰ complex fragment into the C_{aryl}–C_{ethynyl} bond occurs intramolecular or intermolecular in the crystalline state. Taking a closer look to the arrangement of the (diphosphine)(η^2 -tolane)Pt⁰ complexes in the crystal ought to be a simplified estimation concerning this problem. Fig. 4 exemplarily shows the alignment of **5a** in the solid state. The shortest distance between two platinum atoms of neighbouring molecules of **5a** (labeled as **A** and **B**) was determined to be 7.45 Å. The tolane moiety of **B**, highlighted as purple triangle, is evidently not directed to the Pt center of **A**, suggesting that their distance is not significantly shorter than 7.45 Å. Indeed, approximated distances, calculated between the Pt atom of **A** and one of the C_{ethynyl} atoms of **B**, were found to be 7.07 Å and 7.84 Å, respectively. Regarding that typically observed distances among reactive centers in the course of photochemical reactions in the

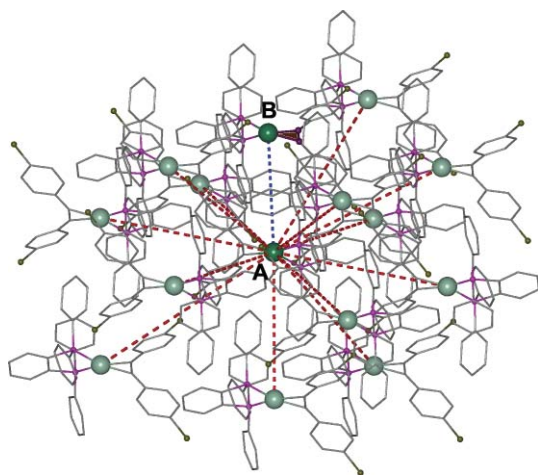


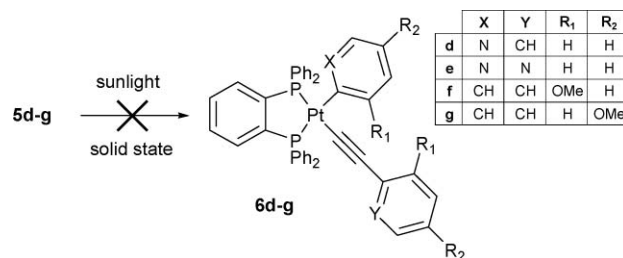
Fig. 4 Section of the crystal-state arrangement of **5a**. Platinum atoms are depicted as green colored spheres. Intermolecular Pt...Pt distances are represented by dashed lines, whereas red lines exhibit a length of approximately 10–13 Å and the shortest contact (7.45 Å) is emphasized by a blue colored dashed line.

solid state are generally in the range of 4 Å,¹⁸ a bimolecular reaction mechanism can be excluded. However, an intramolecular attack of the (diphosphine)Pt moiety on the C_{aryl}–C_{ethynyl} bond after a photo-excitation of **5a** (see Part B†) seems to be more plausible due to the close proximity of the Pt atom to the regarded bond. This might result in a reduced activation barrier for C–C bond activation and explains the high selectivity in the solid state. The determined intermolecular Pt...Pt distances of complexes **5b–5g** and **9a–b** are comparable to those of **5a**. Therefore, an expansion of the postulated mechanism of the solid state C–C bond activation to these complexes ought to be justified.

On the contrary, the formation of the C–Br activated compound **7a** via irradiating **5a** in solution can be reasonably explained by a “ring-walking” mechanism of the (diphosphine)Pt moiety along the π-system of the tolane ligand as similarly described for bromo substituted stilbene and azostilbene derivatives coordinated to a (PEt₃)₂Ni¹⁹ as well as (PEt₃)₂Pt complex fragment.²⁰

The photochemical conversions of **5a–c** to their C–C activated counterparts suggest that the reactivity towards C–C bond cleavage in the solid state obviously depends on the electronic nature of the used tolane ligand as well as on the spatial orientation of its phenyl groups (for a detailed explanation see Part B†). In view of a minimization of potential steric influences, complexes **5d** and **5e** have been synthesized. The decreased steric bulkiness of the pyridyl groups allows an almost coplanar arrangement in the corresponding complexes, as reflected by the torsion angles of 6.4° and 26.9° found for complexes **5d** and **5e**, respectively (Table 1). Therefore, crystalline samples of **5d** and **5e** were placed in the sunlight for approximately two weeks. After this period, no obvious alterations of these samples were observed. Their ³¹P{¹H} NMR spectra revealed the signals of the starting material unchanged, indicating that no photoreaction occurred (Scheme 5).

The photolysis of **5d** and **5e** in solution resulted in the formation of some unidentified side products. No signals assignable to the corresponding C–C activated products have been detected in the appropriate ³¹P{¹H} NMR spectra.

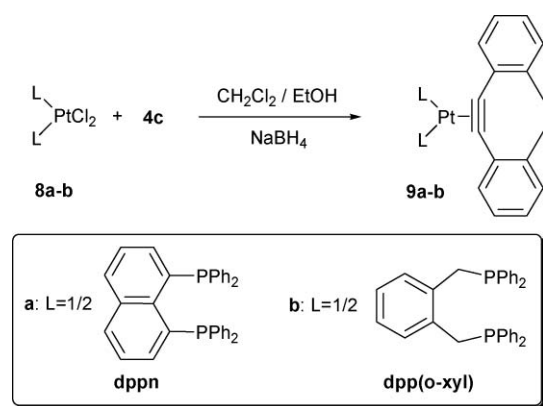


Scheme 5 Complexes **5d–g** are non-reactive towards sunlight in the solid state.

In order to study the influence of EDGs attached to the tolane ligand, complexes **5f** and **5g** were placed in the sunlight for photoreactions. However, neither **5f** nor **5g** showed any rearrangement towards C–C or C–O bond activation with respect to the ³¹P{¹H} NMR spectroscopic data (Scheme 5). These results suggest an inhibition of C–C bond cleavage in the solid state by the presence of EDGs on the tolane moiety. Furthermore, in the case of **5f**, this inhibition-effect seems to be stronger than a potential C–C bond activation arising from the spatial orientation of the phenyl rings, because its dihedral angle ought to be in the same range as observed for the other complexes bearing *ortho*-substituted tolanes. Single crystals of **5f** and **5g** were of poor quality and not suitable for X-ray structure determination. Hence, no information of the alignment of the phenyl groups in the solid state is available. However, some information can be extracted from the theoretical optimized geometries of **5f** and **5g**, which predict C(8)–C(3)–C(9)–C(14) torsion angles of 72.2° and 20.1°, respectively. Due to its greater torsion angle, in comparison with **5g**, we expect complex **5f** to be prone in view of C–C bond activation. Accordingly, the photolysis of **5f** in toluene solution resulted in the predominant formation of **6f**, which was verified by the presence of an AB spin system pattern accompanied with ¹⁹⁵Pt satellites (49.5/47.6 ppm, ¹J_{Pt} = 2473/1687 Hz) in the ³¹P{¹H} NMR spectrum. The reaction of **5g** under similar conditions revealed almost no conversion into the corresponding insertion product **6g**, based on the ³¹P{¹H} NMR spectroscopic data. However, attempts to isolate compounds **6f** and **6g** by means of column chromatography failed.

In order to investigate the influence of the bridging diphosphine ligand on the reactivity, we focused on one tolane ligand (**4c**) and synthesized two additional Pt⁰ complexes (**9a–b**) with diphosphine ligands promising different bite angles P–Pt–P. Compounds **9a** and **9b** were prepared by reduction of the appropriate Pt^{II} metal precursor (**8a–b**) with sodium borohydride in dichloromethane–ethanol solution and subsequent treatment with **4c** (Scheme 6). Diffusion of pentane into saturated benzene solutions of the crude products afforded orange (**9a**) and pale yellow (**9b**) crystals in analytical purity. The ³¹P{¹H} NMR spectra of **9a** and **9b** show a singlet with ¹⁹⁵Pt satellites at 17.4 and 13.6 ppm, respectively. Interestingly, the ¹J_{Pt} values increase with the corresponding bite angles of the diphosphines. A similar correlation between these values was already observed in related systems.^{14,21,22}

The molecular arrangements of **9a** and **9b** were unambiguously confirmed by the results of the X-ray structure determination (Fig. 5 and 6). Both complexes exhibit a distorted square-planar coordination geometry. Selected bond lengths and angles are summarized in Table 1 and comparable with those determined



Scheme 6 Synthesis of (diphosphine)(η^2 -2,2'-dimethyltolane)Pt⁰ complexes **9a–b**, bearing diphosphines with different bite angles.

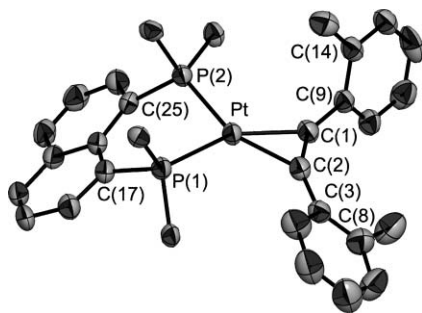


Fig. 5 Molecular structure of **9a** with thermal ellipsoids at 50% probability level. Hydrogen atoms and solvent molecules have been omitted for clarity. The phenyl groups of the 1,8-bis(diphenylphosphanyl)naphthalene ligand (dppn) are represented by their *ipso*-carbon atoms. Selected bond lengths and angles are summarized in Table 1.

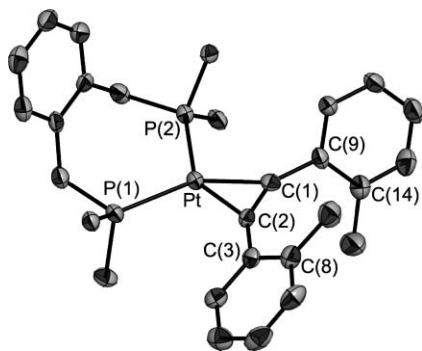
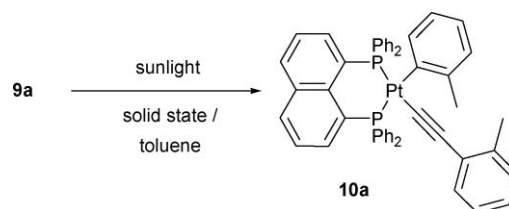


Fig. 6 Molecular structure of **9b** with thermal ellipsoids at 50% probability level. Hydrogen atoms and solvent molecules have been omitted for clarity. The phenyl groups of the α,α' -bis(diphenylphosphanyl)-*o*-xylene [dpp(*o*-xyl)] ligand are represented by their *ipso*-carbon atoms. Selected bond lengths and angles are summarized in Table 1.

for **5a–e**, except the angles P(1)–Pt–P(2) which are predetermined by the particular diphosphine. The torsion angle of the phenyl rings of the tolane ligand in **9b** was experimentally determined to be 75.6°, which is in good agreement with the theoretically calculated value of 72.5° (Table 1) and thus, is comparable to that in **5c**. In contrast, the appropriate angle in **9a** was found to be significantly enlarged to 121.9°.

If crystals of **9a** are irradiated with sunlight for two weeks, smooth fading of the orange color was observed pointing to

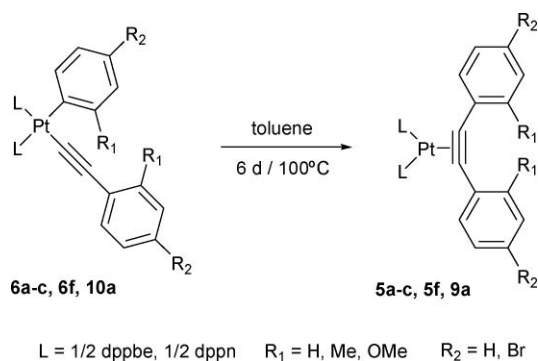
a photochemical induced reaction. Indeed, the $^{31}\text{P}\{^1\text{H}\}$ NMR spectrum of this sample displayed full conversion of **9a** to an unsymmetrical complex characterized by two doublets at 11.9 and 9.0 ppm. The $^1J_{\text{P,Pt}}$ values (2427/1499 Hz) are comparable to those determined for **6a–c**, pointing to the formation of **10a** (Scheme 7). The IR spectrum of **10a** shows strong absorption at $\nu = 2112\text{ cm}^{-1}$, typical for an end-on coordinated alkyne ligand. In contrast, a crystalline sample of **9b**, which was placed in sunlight for a similar period, did not show any visible alterations as confirmed by the unchanged $^{31}\text{P}\{^1\text{H}\}$ NMR spectrum.



Scheme 7 The dppn complex **9a** shows light induced selective C–C bond cleavage in the crystalline state as well as in solution.

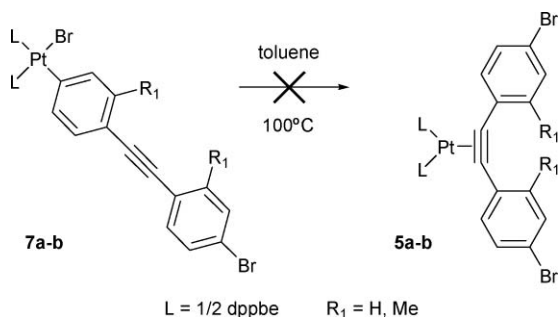
The exposure of a toluene solution of **9a** to the sunlight resulted in the exclusive formation of **10a**, as can be followed by $^{31}\text{P}\{^1\text{H}\}$ NMR spectroscopy. On the contrary, the $^{31}\text{P}\{^1\text{H}\}$ NMR spectrum of a solution of **9b**, irradiated with sunlight for several days, indicates almost no conversion of **9b** except for a small amount of the dioxidized phosphine ligand (33.0 ppm). On the one hand, the differences in the reactivity of **9a/9b** in solid state and solution might be explained by the remarkably different torsion angles of the phenyl rings of the coordinated **4c**. On the other hand, a clear trend in the relation between the phosphine chelate ring size (and hence the bite angle P–Pt–P) and the reactivity is evident. Whereas **5c** and **9a**, realizing 5- and 6-membered chelate rings, respectively, and exhibiting relatively small P–Pt–P angles (86–88°), are reactive towards sunlight in the solid state and in solution, **9b** proved to be unreactive under similar conditions, as mentioned above. This complex exhibits a 7-membered chelate ring with an appropriate P–Pt–P angle of almost 103°. These miscellaneous diphosphines are known to influence the electronic nature of the appropriate Pt⁰ fragment,²³ what might explain the different reactivity of complexes **5c**, **9a** and **9b** in the solid state and in solution, respectively. A detailed discussion concerning the factors influencing the reactivity is given in Part B.‡

Generally, the described photochemically induced C–C bond activation is thermodynamically uphill, hence the reactivity is reversible under thermal conditions. In order to prove this assumption for the specified complexes **5a–c**, **5f** and **9a**, which show C–C bond activation, their thermal induced back reactions were investigated (for mechanistic DFT studies see Part B.‡). Therefore, toluene-*d*₈ solutions of **5a–c**, **5f** and **9a** were placed in NMR tubes and exposed to sunlight. After 10 days the formation of the corresponding Pt^{II} counterparts was confirmed by $^{31}\text{P}\{^1\text{H}\}$ NMR spectroscopy and thereupon the NMR tubes were sealed and placed in an oil bath at 100 °C. After 6 days a $^{31}\text{P}\{^1\text{H}\}$ NMR spectrum of each sample was recorded. The $^{31}\text{P}\{^1\text{H}\}$ NMR spectroscopic data of the experiments on **5c**, **5f** and **9a** revealed the quantitative re-conversion of the photochemically generated Pt^{II} complexes **6c**, **6f** and **10a** into the appropriate Pt⁰ complexes (Scheme 8).



Scheme 8 Photochemical C–C bond cleavage in (diphosphine)(η^2 -tolane)Pt⁰ complexes is reversible under thermal conditions.

If 1 : 1 mixtures of **6a** and **7a** as well as **6b** and **7b**, obtained by irradiating solutions of **5a** and **5b** with sunlight, respectively, are treated in a similar manner, the ³¹P{¹H} NMR spectra only revealed the re-conversion of **6a** and **6b** into **5a** and **5b** (Scheme 8), whereas the signals of **7a** and **7b** remained unchanged. This underlines the irreversible light induced oxidative addition of the C–Br bond to the (diphosphine)Pt⁰ moiety in **5a** and **5b**, respectively (Scheme 9). The irreversibility of the C–Br bond activation reaction is addressed in Part B,[‡] where mechanistic DFT studies show that the appropriate backwards thermal reductive elimination is thermodynamically uphill.



Scheme 9 Complexes **7a** and **7b** are stable towards higher temperatures and show no rearrangement to **5a** and **5b**, respectively.

Conclusions

In summary, we were able to extend our previously reported simple and straightforward synthesis of (diphosphine)(tolane)Pt⁰ complexes to a new series of complexes (**5a–g** and **9a–b**), bearing tolane ligands with manifold substituent patterns. Comparison of their reactivity towards C–C bond activation showed that on the one hand the spatial orientation of the phenyl rings of the tolane ligand and on the other hand the electronic properties of substituents attached to the tolane moiety influence the light induced intramolecular oxidative addition of the C_{aryl}–C_{ethynyl} bond to the Pt⁰ moiety in the crystalline state as well as in solution. While compounds **5d–g**, exhibiting either a relatively small twisting of the phenyl or pyridyl rings of the tolane ligand or strong EDGs, are unreactive towards sunlight, complexes **5a–c** and **9a** could be selectively converted to the appropriate C–C activated counterparts. Additionally, solution state photolysis of **5a** and **5b**, bearing bromo substituted tolane ligands, leads to 1 : 1 mixtures of

the C–C activated as well as the C–Br activated complexes **7a** and **7b**. The formation of **7a** and **7b** can be reasonably explained by a “ring walking” mechanism of the Pt⁰ complex fragment on the π -system of the ligand resulting in C–Br bond activation. However, the highly selective formation of the C–C activated complexes in the crystalline state might be caused by the close proximity of both reactive sites of the appropriate complex. The observed C–C bond cleavage proved to be reversible under thermal conditions, whereas the insertion of the Pt⁰ complex fragment in the C–Br bonds turned out to be irreversible, pointing to the thermal stability of complexes **7a** and **7b**, respectively.

In order to render the mechanism of this bond cleavage in the crystalline state precisely, more information about the excited states in the course of the reactions are indispensable. Therefore, results of theoretical calculations on the UV-spectra of the (diphosphine)(η^2 -tolane)Pt⁰ complexes are presented in Part B of this work,[‡] which should substantiate the factors influencing the different reactivity towards C–C bond cleavage.

Experimental section

General considerations

Unless otherwise stated, all reactions were carried out under an atmosphere of argon by using standard Schlenk techniques. All chemicals were purchased from commercial suppliers and used without further purification. The starting materials (dppbe)PtCl₂ (**3**),²⁴ (dppn)PtCl₂ (**8a**),²⁵ (dpp(o-xy))PtCl₂ (**8b**)²⁶ as well as the tolane derivatives **4d**²⁷ and **4e**²⁷ were prepared according to literature procedures. Compounds **4a**,²⁸ **4c**,²⁹ **4f**³⁰ and **4g**³⁰ are known from literature and were synthesized in a similar manner as the synthesis of **4b** described below. The determined spectroscopic data are in good agreement with the reported ones. The NMR spectra were recorded either with BRUKER AVANCE 400 or BRUKER AVANCE 200 spectrometers at 27 °C. ¹H NMR spectra were calibrated using the signal of the residual non-deuterated solvent, while ¹³C{¹H} NMR spectra were measured using the signal of the solvent as internal standard. ³¹P{¹H} NMR spectra were determined using 85% H₃PO₄ as external standard. The assignment of the signals in the ¹H and ¹³C{¹H} NMR spectra of compounds **5a–g** and **9a–b** was performed by means of two-dimensional NMR methods (¹H,¹H-COSY, ¹H,¹³C-HSQC and ¹H,¹³C-HMBC). The protons as well as carbon atoms of the appropriate tolane ligand are labeled according to Scheme 2, whereas the signals of the ethynyl carbon atoms could not be detected due to their low intensity. The complexity of the ¹H and ¹³C{¹H} NMR spectra of compounds **6a**, **7a**, **7b** and **10a** disabled an exact assignment for most of the signals, even by applying two-dimensional NMR methods. Mass spectra were taken with a FINNIGAN MAT SSQ 710 mass spectrometer. IR spectra were recorded with a PERKIN ELMER system 2000 FT-IR spectrometer. Elemental analyses were performed with a Vario EL III CHNS (Elementaranalysen GmbH Hanau) as single determinations. Melting points were determined using an AXIOLAB microscope with a THMS 600 heating plate and are uncorrected.

2,2'-dimethyl-4,4'-dibromotolane (4b). To a solution of 2-iodo-5-bromotoluene (4.43 g, 14.9 mmol) in Et₃N (40 mL) trimethylsilylacetylene (1.48 g, 15.1 mmol), copper(I)iodide (117 mg,

0.61 mmol) and $(\text{PPh}_3)_2\text{PdCl}_2$ (126 mg, 0.18 mmol) were added, whereupon the color of the solution turned to black and triethylammoniumiodide began to precipitate. After stirring for 5 days the solid was filtered through Celite[®] and the residue was rinsed with diethyl ether. The combined solvents were removed under reduced pressure to give a dark oil which was distilled *in vacuo* to give 2-trimethylsilylethynyl-5-bromotoluene³¹ as colorless oil. (3.42 g, 88%); δ_{H} (200 MHz, CDCl_3) 7.35–7.18 (m, 3 H), 2.37 (s, 3 H), 0.23 (s, 9 H); δ_{C} (50 MHz, CDCl_3) 142.6 (s), 133.3 (s), 132.3 (s), 128.6 (s), 122.5 (s), 122.0 (s), 102.9 (s), 99.6 (s), 20.4 (s), 0.0 (s).

A solution of 2-trimethylsilylethynyl-5-bromotoluene (2.50 g, 9.34 mmol) in thf (30 mL) was cooled to -78°C and tetra-*n*-butylammoniumfluoride, dissolved in thf (20 mL), was added drop wise. After warming to room temperature the yellow solution was stirred over night. Then the solution was washed three times with water, the phases were separated and the organic layer was dried over Na_2SO_4 . The solvent was removed under reduced pressure to yield 2-ethynyl-5-bromotoluene as pale yellow oil. (1.70 g, 93%); δ_{H} (200 MHz, CDCl_3) 7.34–7.21 (m, 3 H), 3.28 (s, 1 H), 2.37 (s, 3 H); δ_{C} (50 MHz, CDCl_3) 142.8 (s), 133.7 (s), 132.4 (s), 128.8 (s), 122.8 (s), 120.9 (s), 82.0 (s), 81.5 (s), 20.4 (s).

To a solution of 2-ethynyl-5-bromotoluene (1.70 g, 8.72 mmol) in Et_3N (40 mL) 2-iodo-5-bromotoluene (2.61 g, 8.80 mmol), copper(i)iodide (113 mg, 0.59 mmol) and $(\text{PPh}_3)_2\text{PdCl}_2$ (104 mg, 0.15 mmol) were added, whereas the color of the solution turned black and triethylammoniumiodide began to precipitate. After stirring for 5 days the solvent was removed *in vacuo*. The residue was dissolved in CH_2Cl_2 and washed with water, saturated NH_4Cl solution and again water and dried over Na_2SO_4 . After removing the solvent the crude product was recrystallized from ethanol to yield **4b** as white solid (2.06 g, 65%). Mp: 119–120 $^\circ\text{C}$; δ_{H} (200 MHz, CDCl_3) 7.41 (m, 2 H), 7.33–7.28 (m, 4 H), 2.48 (s, 6 H); δ_{C} (50 MHz, CDCl_3) 141.9 (s), 133.1 (s), 132.5 (s), 128.9 (s), 122.4 (s), 122.0 (s), 92.3 (s), 20.7 (s); Anal. calcd. for $\text{C}_{16}\text{H}_{12}\text{Br}_2$: C 52.78, H 3.32, Br 43.89; Found: C 53.14, H 3.30, Br 43.72.

General procedure for the syntheses of the (diphosphine) $(\eta^2\text{-tolane})\text{Pt}^0$ complexes

The appropriate (diphosphine) PtCl_2 was suspended in CH_2Cl_2 (12 mL) and ethanol (3 mL) in a Schlenk flask. To this suspension NaBH_4 (50 mg, 1.06 mmol) was added and stirred for 6 h at rt. During this period the mixture became yellow to orange in color and the (diphosphine) PtCl_2 dissolved. Water (5 mL) was added to the mixture and after diminishing of the hydrogen evolution the phases were separated using a pipette and the appropriate tolane ligand was added to the organic layer in equimolar ratio. This solution was stirred over night. After removing the solvent under reduced pressure, the residue was dissolved in a small amount of thf and this solution was filtered through a silica gel charged pipette. The solvent was evaporated and the yellow to orange colored crude product was dissolved in toluene or benzene (3 mL). Pure complexes were obtained by slow diffusion of pentane into these solutions.

[(dppbe)($\eta^2\text{-4,4'$ -dibromotoluene) Pt^0] (5a). Compound **3** (142 mg, 0.20 mmol) was reacted with **4a** (66 mg, 0.20 mmol) to yield **5a** (83 mg, 40%) as orange crystals.

Mp: 127 $^\circ\text{C}$ (dec.); δ_{H} (400 MHz; CD_2Cl_2) 7.77 (m, 2 H, *o*- C_6H_4 of dppbe), 7.59 (m, 8 H, *o*- C_6H_5 of dppbe), 7.48 (m, 2 H, *m*-

C_6H_4 of dppbe), 7.35 (m, 16 H, *m*- C_6H_5 and *p*- C_6H_5 of dppbe and *H*-2/*H*-2' and *H*-6/*H*-6'), 7.26 (m, 4 H, *H*-3/*H*-3' and *H*-5/*H*-5'); δ_{C} (100 MHz, CD_2Cl_2) 146.4 (m, *ipso*- C_6H_4 of dppbe), 135.5 (m, *ipso*- C_6H_5 of dppbe), 134.4 (m, *C*-1/*C*-1'), 134.0 (m, *o*- C_6H_4 of dppbe), 133.3 (m, *o*- C_6H_5 of dppbe), 132.3 (m, *C*-2/*C*-2' and *C*-6/*C*-6'), 131.5 (s, *C*-3/*C*-3' and *C*-5/*C*-5'), 131.2 (s, *m*- C_6H_4 of dppbe), 130.3 (s, *p*- C_6H_5 of dppbe), 128.8 (m, *m*- C_6H_5 of dppbe), 120.1 (s, *C*-4/*C*-4'); δ_{P} (81 MHz, CD_2Cl_2) 51.17 (s with ^{195}Pt satellites, $^1J_{\text{P,Pt}} = 3087$ Hz); $\nu(\text{KBr})/\text{cm}^{-1}$ 3052 (s), 1736 (s, $\nu(\text{C}\equiv\text{C})$), 1629 (s), 1482 (vs), 1434 (vs), 1389 (m), 1097 (vs) 1067 (s), 1008 (s), 826 (s), 745 (s), 694 (vs), 669 (s), 548 (vs), 527 (s); *m/z* (DEI) 976 (2%, $[\text{M}]^+$), 896 (2, $[\text{M} - \text{Br}]^+$), 721 (30, $[(\text{dppbe})\text{PtBr}]^+$), 641 (10, $[(\text{dppbe})\text{Pt}]^+$), 336 (23, **[4a]**⁺); Anal. calcd. for $\text{C}_{44}\text{H}_{32}\text{Br}_2\text{P}_2\text{Pt}$: C 54.06, H 3.30, Br 16.35; Found C 54.30, H 3.51, Br 16.01.

[(dppbe)($\eta^2\text{-2,2'$ -dimethyl-4,4'-dibromotoluene) Pt^0] (5b). Compound **3** (175 mg, 0.25 mmol) was reacted with **4b** (89 mg, 0.24 mmol) to yield **5b** (111 mg, 45%) as yellow crystals.

Mp: $>230^\circ\text{C}$; δ_{H} (400 MHz, CD_2Cl_2) 7.81 (m, 2 H, *o*- C_6H_4 of dppbe), 7.50 (m, 10 H, *m*- C_6H_4 and *o*- C_6H_5 of dppbe), 7.36 (m, 4 H, *p*- C_6H_5 of dppbe), 7.29 (m, 8 H, *m*- C_6H_5 of dppbe), 7.22 (s, 2 H, *H*-3/*H*-3'), 7.00 (m, 4 H, *H*-5/*H*-5' and *H*-6/*H*-6'), 1.96 (s, 6 H, CH_3); δ_{C} (100 MHz, CD_2Cl_2) 146.4 (m, *ipso*- C_6H_4 of dppbe), 138.7 (m, *C*-2/*C*-2'), 137.0 (m, *C*-1/*C*-1'), 135.8 (m, *ipso*- C_6H_5 of dppbe), 134.1 (m, *o*- C_6H_4 of dppbe), 133.1 (m, *o*- C_6H_5 of dppbe), 132.6 (s, *C*-6/*C*-6'), 132.1 (s, *C*-3/*C*-3'), 131.2 (s, *m*- C_6H_4 of dppbe), 130.1 (s, *p*- C_6H_5 of dppbe), 128.7 (m, *m*- C_6H_5 of dppbe), 128.2 (s, *C*-5/*C*-5'), 119.3 (s, *C*-4/*C*-4'), 21.0 (s, CH_3); δ_{P} (81 MHz, CD_2Cl_2) 51.59 (s with ^{195}Pt satellites, $^1J_{\text{P,Pt}} = 3143$ Hz); $\nu(\text{KBr})/\text{cm}^{-1}$ 3052 (m), 2930 (w), 1763 (m, $\nu(\text{C}\equiv\text{C})$), 1625 (m), 1475 (s), 1434 (s), 1188 (m), 1097 (s), 891 (m), 745 (m), 694 (vs), 549 (vs), 527 (vs), 507 (s); *m/z*(DEI) 1006 (2%, $[\text{M}]^+$), 923 (2, $[\text{M} - \text{Br}]^+$), 721 (6, $[(\text{dppbe})\text{PtBr}]^+$), 641 (2, $[(\text{dppbe})\text{Pt}]^+$), 485 (1, $[(\text{dppbe})\text{Pt} - 2\times\text{Ph}]^+$), 364 (3, **[4b]**⁺); Anal. calcd. for $\text{C}_{46}\text{H}_{36}\text{Br}_2\text{P}_2\text{Pt}$: C 54.94, H 3.61, Br 15.89; Found C 55.16, H 3.69, Br 16.01.

[(dppbe)($\eta^2\text{-2,2'$ -dimethyltolane) Pt^0] (5c). Compound **3** (129 mg, 0.18 mmol) was reacted with **4c** (37 mg, 0.18 mmol) to yield **5c** (113 mg, 74%) as orange crystals.

Mp: 132 $^\circ\text{C}$ (dec.); δ_{H} (400 MHz, CD_2Cl_2) 7.81 (m, 2 H, *o*- C_6H_4 of dppbe), 7.52 (m, 8 H, *o*- C_6H_5 of dppbe), 7.45 (m, 2 H, *m*- C_6H_4 of dppbe), 7.34 (m, 4 H, *p*- C_6H_5 of dppbe), 7.28 (m, 8 H, *m*- C_6H_5 of dppbe), 7.15 (d, $^3J_{\text{H,H}} = 7.6$ Hz, 2 H, *H*-6/*H*-6'), 7.07 (d, $^3J_{\text{H,H}} = 7.2$ Hz, 2 H, *H*-3/*H*-3'), 6.98 (t, $^3J_{\text{H,H}} = 7.2$ Hz, 2 H, *H*-4/*H*-4' or *H*-5/*H*-5'), 6.91 (t, $^3J_{\text{H,H}} = 7.2$ Hz, 2 H, *H*-4/*H*-4' or *H*-5/*H*-5'), 2.01 (s, 6 H, CH_3); δ_{C} (100 MHz, CD_2Cl_2) 146.7 (m, *ipso*- C_6H_4 of dppbe), 137.8 (m, *C*-2/*C*-2'), 136.6 (m, *C*-1/*C*-1'), 136.2 (m, *ipso*- C_6H_5 of dppbe), 134.1 (m, *o*- C_6H_4 of dppbe), 133.2 (m, *o*- C_6H_5 of dppbe), 131.3 (s, *C*-6/*C*-6'), 131.0 (s, *m*- C_6H_4 of dppbe), 129.9 (s, *p*- C_6H_5 of dppbe), 129.4 (s, *C*-3/*C*-3'), 128.6 (m, *m*- C_6H_5 of dppbe), 125.9 (s, *C*-4/*C*-4' or *C*-5/*C*-5'), 125.2 (s, *C*-4/*C*-4' or *C*-5/*C*-5'), 21.2 (s, CH_3); δ_{P} (81 MHz, CD_2Cl_2) 52.05 (s with ^{195}Pt satellites, $^1J_{\text{P,Pt}} = 3138$ Hz); $\nu(\text{KBr})/\text{cm}^{-1}$ 3052 (s), 2922 (m), 1778 (m, $\nu(\text{C}\equiv\text{C})$), 1753 (m), 1625 (s), 1481 (s), 1434 (vs), 1096 (s), 759 (s) 694 (vs), 547 (vs), 527 (vs); *m/z*(DEI) 847 (100%, $[\text{M}]^+$), 641 (60, $[(\text{dppbe})\text{Pt}]^+$), 486 (10, $[(\text{dppbe})\text{Pt} - 2\times\text{Ph}]^+$), 205 (20, **[4c]**⁺); Anal. calcd. for $\text{C}_{46}\text{H}_{38}\text{P}_2\text{Pt}$: C 65.17, H 4.52; Found C 64.88, H 4.46.

[(dppbe)(η^2 -1-phenyl-2-(2-pyridyl)acetylene)Pt⁰] (**5d**). Compound **3** (112 mg, 0.16 mmol) was reacted with **4d** (29 mg, 0.16 mmol) to yield **5d** (54 mg, 49%) as yellow crystals.

Mp: 138 °C (dec.); δ_{H} (400 MHz, CD₂Cl₂) 8.61 (d, ³J_{H,H} = 4.2 Hz, 1 H, *H*-5), 7.99 (d, ³J_{H,H} = 7.0 Hz, 2 H, *H*-2'/*H*-6'), 7.79 (m, 2 H, *o*-C₆H₄ of dppbe), 7.67 (m, 8 H, *o*-C₆H₅ of dppbe), 7.48 (m, 2 H, *m*-C₆H₄ of dppbe), 7.33 (m, 13 H, *m*-C₆H₅ and *p*-C₆H₅ of dppbe and *H*-3), 7.25 (d, ³J_{H,H} = 7.7 Hz, 1 H, *H*-2), 7.16 (m, 3 H, *H*-3', *H*-4' and *H*-5'), 6.97 (m, 1 H, *H*-4); δ_{C} (100 MHz, CD₂Cl₂) 154.6 (m, *C*-1), 149.8 (s, *C*-5), 146.4 (m, *ipso*-C₆H₄ of dppbe), 136.2 (s, *C*-3), 135.5 (m, *ipso*-C₆H₅ of dppbe), 134.0 (m, *o*-C₆H₄ of dppbe and *C*-1'), 133.4 (m, *o*-C₆H₅ of dppbe), 132.7 (m, *C*-2' and *C*-6'), 131.1 (s, *m*-C₆H₄ of dppbe), 130.2 (s, *p*-C₆H₅ of dppbe), 128.7 (m, *m*-C₆H₅ of dppbe), 128.3 (s, *C*-3' and *C*-5'), 127.4 (s, *C*-2), 127.2 (s, *C*-4'), 120.4 (s, *C*-4); δ_{P} (81 MHz, CD₂Cl₂) 51.28 (d with ¹⁹⁵Pt satellites, ¹J_{Pt} = 3063 Hz, ²J_{Pt} = 55.1 Hz), 51.25 (d with ¹⁹⁵Pt satellites, ¹J_{Pt} = 3079 Hz, ²J_{Pt} = 55.1 Hz); ν (KBr)/cm⁻¹ 3051 (s), 1736 (s, ν (C≡C)), 1629 (s), 1579 (vs), 1555 (m), 1482 (s), 1435 (vs), 1424 (vs), 1097 (vs), 759 (s), 694 (vs), 669 (s), 548 (vs), 527 (vs); *m/z*(FAB in nba) 821 (80%, [M]⁺), 641 (65, [(dppbe)Pt]⁺), 561 (55, [(dppbe)Pt - Ph]⁺), 485 (75, [(dppbe)Pt - 2×Ph]⁺); Anal. calcd. for C₄₃H₃₃N₂Pt · C₄H₈O: C 63.22, H 4.63, N 1.57; Found C 63.26, H 4.67, N 1.56.

[(dppbe)(η^2 -1,2-bis(2-pyridyl)acetylene)Pt⁰] (**5e**). Compound **3** (133 mg, 0.19 mmol) was reacted with **4e** (34 mg, 0.19 mmol) to yield **5e** (75 mg, 49%) as yellow crystals.

Mp: 165 °C (dec.); δ_{H} (400 MHz, CD₂Cl₂) 8.53 (m, 2 H, *H*-5/*H*-5'), 7.96 (d, ³J_{H,H} = 7.8 Hz, 2 H, *H*-2/*H*-2'), 7.84 (m, 2 H, *o*-C₆H₄ of dppbe), 7.74 (m, 8 H, *o*-C₆H₅ of dppbe), 7.49 (m, 4 H, *m*-C₆H₄ of dppbe and *H*-3/*H*-3'), 7.33 (m, 12 H, *m*-C₆H₅ and *p*-C₆H₅ of dppbe), 7.01 (m, 2 H, *H*-4/*H*-4'); δ_{C} (100 MHz, CD₂Cl₂) 153.5 (m, *C*-1/*C*-1'), 149.7 (s, *C*-5/*C*-5'), 146.5 (m, *ipso*-C₆H₄ of dppbe), 136.1 (s, *C*-3/*C*-3'), 135.9 (m, *ipso*-C₆H₅ of dppbe), 134.2 (m, *o*-C₆H₄ of dppbe), 133.5 (m, *o*-C₆H₅ of dppbe), 131.1 (s, *m*-C₆H₄ of dppbe), 130.1 (s, *p*-C₆H₅ of dppbe), 128.6 (m, *m*-C₆H₅ of dppbe), 127.4 (m, *C*-2/*C*-2'), 121.0 (s, *C*-4/*C*-4'); δ_{P} (81 MHz, CD₂Cl₂) 52.60 (s with ¹⁹⁵Pt satellites, ¹J_{Pt} = 3108 Hz); ν (KBr)/cm⁻¹ 3049 (s), 1736 (s, ν (C≡C)), 1628 (m), 1579 (vs), 1556 (s), 1481 (s), 1461 (vs), 1434 (vs), 1425 (vs), 1272 (m), 1097 (s), 781 (s), 744 (s), 694 (vs), 549 (vs), 527 (vs); *m/z*(FAB in nba) 822 (25%, [M]⁺), 641 (15, [(dppbe)Pt]⁺), 561 (15, [(dppbe)Pt - Ph]⁺), 485 (40, [(dppbe)Pt - 2×Ph]⁺), 408 (40, [(dppbe)Pt - 3×Ph]⁺); Anal. calcd. for C₄₂H₃₂N₂Pt: C 61.39, H 3.93, N 3.41; Found C 61.54, H 3.81, N 3.35.

[(dppbe)(η^2 -2,2'-dimethoxytolane)Pt⁰] (**5f**). Compound **3** (129 mg, 0.18 mmol) was reacted with **4f** (43 mg, 0.18 mmol) to yield **5f** (54 mg, 34%) as yellow crystals.

Mp: 183 °C (dec.); δ_{H} (400 MHz, CD₂Cl₂) 7.79 (m, 2 H, *o*-C₆H₄ of dppbe), 7.60 (m, 8 H, *o*-C₆H₅ of dppbe), 7.45 (m, 2 H, *m*-C₆H₄ of dppbe), 7.29 (m, 12 H, *m*-C₆H₅ and *p*-C₆H₅ of dppbe), 7.11 (m, 2 H, *H*-6/*H*-6'), 7.07 (t, ³J_{H,H} = 7.2 Hz, 2 H, *H*-4/*H*-4'), 6.77 (d, ³J_{H,H} = 8.4 Hz, 2 H, *H*-3/*H*-3'), 6.67 (t, ³J_{H,H} = 7.2 Hz, 2 H, *H*-5/*H*-5'), 3.43 (s, 6 H, OCH₃); δ_{C} (100 MHz, CD₂Cl₂) 157.6 (s, *C*-2/*C*-2'), 146.9 (m, *ipso*-C₆H₄ of dppbe), 136.3 (m, *ipso*-C₆H₅ of dppbe), 134.0 (m, *o*-C₆H₄ of dppbe), 133.3 (m, *o*-C₆H₅ of dppbe), 133.1 (s, *C*-6/*C*-6'), 130.9 (s, *m*-C₆H₄ of dppbe), 129.9 (s, *p*-C₆H₅ of dppbe), 128.6 (m, *m*-C₆H₅ of dppbe), 127.1 (s, *C*-4/*C*-4'), 126.6 (m, *C*-1/*C*-1'), 119.8 (s, *C*-5/*C*-5'), 110.0 (s, *C*-3/*C*-3'), 55.0 (s,

OCH₃); δ_{P} (81 MHz, CD₂Cl₂) 51.68 (s with ¹⁹⁵Pt satellites, ¹J_{Pt} = 3107 Hz); ν (KBr)/cm⁻¹ 3052 (s), 2935 (m), 2830 (m), 1785 (m, ν (C≡C)), 1625 (s), 1587 (s), 1571 (s), 1481 (vs), 1433 (vs), 1241 (vs), 1181 (s), 1096 (vs), 1027 (s), 747 (vs), 695 (vs), 548 (vs), 526 (vs), 507 (vs); *m/z*(DEI) 879 (1%, [M]⁺), 641 (3, [(dppbe)Pt]⁺), 485 (2, [(dppbe)Pt - 2×Ph]⁺), 238 (100, [4f]⁺); Anal. calcd. for C₄₆H₃₈O₂Pt · 0.5 C₇H₈: C 64.21, H 4.57; Found C 63.98, H 4.81.

[(dppbe)(η^2 -4,4'-dimethoxytolane)Pt⁰] (**5g**). Compound **3** (140 mg, 0.20 mmol) was reacted with **4g** (46 mg, 0.20 mmol) to yield **5g** (68 mg, 39%) as orange crystals.

Mp: >230 °C; δ_{H} (400 MHz, CD₂Cl₂) 7.79 (m, 2 H, *o*-C₆H₄ of dppbe), 7.65 (m, 8 H, *o*-C₆H₅ of dppbe), 7.48 (m, 6 H, *m*-C₆H₄ of dppbe and *H*-2/*H*-2' and *H*-6/*H*-6'), 7.34 (m, 12 H, *m*-C₆H₅ and *p*-C₆H₅ of dppbe), 6.68 (m, 4 H, *H*-3/*H*-3' and *H*-5/*H*-5'), 3.76 (s, 6 H, OCH₃); δ_{C} (100 MHz, CD₂Cl₂) 158.5 (s, *C*-4/*C*-4'), 146.9 (m, *ipso*-C₆H₄ of dppbe), 136.0 (m, *ipso*-C₆H₅ of dppbe), 134.0 (m, *o*-C₆H₄ of dppbe), 133.4 (m, *o*-C₆H₅ of dppbe), 132.4 (s, *C*-2/*C*-2' and *C*-6/*C*-6'), 131.0 (s, *m*-C₆H₄ of dppbe), 130.1 (s, *p*-C₆H₅ of dppbe), 128.7 (m, *m*-C₆H₅ of dppbe), 128.0 (m, *C*-1/*C*-1'), 113.8 (s, *C*-3/*C*-3' and *C*-5/*C*-5'), 55.6 (s, OCH₃); δ_{P} (81 MHz, CD₂Cl₂) 51.63 (s with ¹⁹⁵Pt satellites, ¹J_{Pt} = 3065 Hz); ν (KBr)/cm⁻¹ 3052 (s), 2954 (m), 2834 (m), 1743 (m, ν (C≡C)), 1601 (s), 1506 (vs), 1481 (s), 1435 (vs), 1285 (s), 1242 (vs), 1180 (s), 1097 (s), 1028 (s), 831 (s), 747 (s), 694 (vs), 669 (s), 546 (vs), 526 (vs), 506 (s); *m/z*(DEI) 879 (1%, [M]⁺), 641 (3, [(dppbe)Pt]⁺), 486 (1, [(dppbe)Pt - 2×Ph]⁺), 238 (100, [4g]⁺); Anal. calcd. for C₄₆H₃₈O₂Pt: C 62.80, H 4.35; Found C 62.46, H 4.36.

[(dppn)(η^2 -2,2'-dimethyltolane)Pt⁰] (**9a**). Compound **8a** (235 mg, 0.31 mmol) was reacted with **4c** (64 mg, 0.31 mmol) to yield **9a** (175 mg, 63%) as orange crystals.

Mp: 106 °C (dec.); δ_{H} (400 MHz, CD₂Cl₂) 8.02 (dd, ³J_{H,H} = 8.0 Hz, ⁴J_{H,H} = 1.2 Hz, 2 H, *H*-4 and *H*-5 of dppn), 7.46 (m, 2 H, *H*-2 and *H*-7 of dppn), 7.39 (t, ³J_{H,H} = 7.5 Hz, 2 H, *H*-3 and *H*-6 of dppn), 7.14 (m, 12 H, *o*-C₆H₅ and *p*-C₆H₅ of dppn), 7.02 (m, 8 H, *m*-C₆H₅ of dppn), 6.94 (m, 2 H, *H*-6/*H*-6'), 6.88 (dt, ³J_{H,H} = 7.4 Hz, ⁴J_{H,H} = 1.5 Hz, 2 H, *H*-5/*H*-5'), 6.73 (m, 2 H, *H*-3/*H*-3'), 6.70 (m, 2 H, *H*-4/*H*-4'), 1.98 (s, 6 H, CH₃); δ_{C} (50 MHz, CD₂Cl₂) 139.1 (m, *C*-8a of dppn), 136.9 (m, *C*-2 and *C*-7 of dppn and *C*-2/*C*-2'), 136.2 (m, *ipso*-C₆H₅ of dppn), 135.9 (m, *C*-1 and *C*-8 of dppn and *C*-1/*C*-1'), 133.6 (m, *o*-C₆H₅ of dppn), 132.8 (s, *C*-4 and *C*-5 of dppn), 130.0 (s, *C*-3/*C*-3'), 129.3 (s, *p*-C₆H₅ of dppn), 128.2 (m, *m*-C₆H₅ of dppn), 127.8 (m, *C*-4a of dppn), 125.2 (m, *C*-3 and *C*-6 of dppn and *C*-4/*C*-4' and *C*-5/*C*-5'), 21.2 (s, CH₃); δ_{P} (81 MHz, CD₂Cl₂) 17.43 (s with ¹⁹⁵Pt satellites, ¹J_{Pt} = 3049 Hz); ν (KBr)/cm⁻¹ 3053 (s), 2952 (m), 2919 (m), 1775 (s, ν (C≡C)), 1751 (s, ν (C≡C)), 1595 (s), 1479 (vs), 1455 (s), 1434 (vs), 1313 (m), 1182 (m), 1093 (vs), 875 (m), 824 (m), 772 (vs), 744 (vs), 693 (vs), 587 (vs), 519 (vs), 495 (vs); *m/z*(FAB in nba) 898 (2%, [M]⁺), 691 (6, [(dppn)Pt]⁺), 535 (4, [(dppn)Pt - 2×Ph]⁺); Anal. calcd. for C₅₀H₄₀Pt · C₅H₁₂: C 68.10, H 5.40; Found C 67.91, H 5.25.

[(dpp(o-xy))(η^2 -2,2'-dimethyltolane)Pt⁰] (**9b**). Compound **8b** (140 mg, 0.19 mmol) was reacted with **4c** (40 mg, 0.19 mmol) to yield **9b** (63 mg, 38%) as pale yellow crystals.

Mp: 203 °C (dec.); δ_{H} (400 MHz, CD₂Cl₂) 7.60 (m, 8 H, *o*-C₆H₅ of dpp(o-xy)), 7.36 (m, 4 H, *p*-C₆H₅ of dpp(o-xy)), 7.29 (m, 8 H, *m*-C₆H₅ of dpp(o-xy)), 6.93 (d, ³J_{H,H} = 7.5 Hz, 2 H, *H*-6/*H*-6'), 6.81 (dt, ³J_{H,H} = 7.3 Hz, ⁴J_{H,H} = 1.7 Hz, 2 H, *H*-5/*H*-5'), 6.74

(m, 2 H, *m*-C₆H₄ of dpp(o-xyl)), 6.63 (m, 2 H, *H*-4/*H*-4'), 6.60 (m, 2 H, *H*-3/*H*-3'), 6.25 (m, 2 H, *o*-C₆H₄ of dpp(o-xyl)), 4.13 (m, 4 H, PCH₂), 1.82 (s, 6 H, CH₃); δ_c (100 MHz, CD₂Cl₂) 137.4 (m, *C*-2/*C*-2'), 136.8 (m, *ipso*-C₆H₅ of dpp(o-xyl)), 135.9 (m, *C*-1/*C*-1'), 134.8 (s, *ipso*-C₆H₄ of dpp(o-xyl)), 133.7 (m, *o*-C₆H₅ of dpp(o-xyl)), 131.2 (s, *o*-C₆H₄ of dpp(o-xyl)), 129.9 (s, *p*-C₆H₅ of dpp(o-xyl)), 129.6 (s, *C*-3/*C*-3'), 129.1 (s, *C*-6/*C*-6'), 128.2 (m, *m*-C₆H₅ of dpp(o-xyl)), 126.1 (s, *m*-C₆H₄ of dpp(o-xyl)), 125.3 (s, *C*-5/*C*-5'), 124.8 (s, *C*-4/*C*-4'), 38.9 (m, PCH₂), 21.0 (s, CH₃); δ_p (81 MHz, CD₂Cl₂) 13.58 (s with ¹⁹⁵Pt satellites, ¹*J*_{Pt} = 3449 Hz); ν (KBr)/cm⁻¹ 3053 (s), 2943 (m), 2916 (m), 1779 (s, ν (C≡C)), 1754 (m, ν (C≡C)), 1595 (s), 1480 (vs), 1455 (s), 1435 (vs), 1183 (m), 1096 (vs), 1027 (m), 863 (s), 837 (s), 763 (vs), 742 (vs), 695 (vs), 503 (vs); *m/z*(FAB in nba) 876 (1%, [M]⁺), 669 (4, [(dpp(o-xyl))Pt]⁺); Anal. calcd. for C₄₈H₄₂P₂Pt · C₆H₆: C 67.99, H 5.07; Found C 67.52, H 5.38.

Irradiation experiments in the solid state

In a sample vial the appropriate (diphosphine)(η²-tolane)Pt⁰ complex was placed in the sunlight for the stated periods. From time to time the vial was turned to ensure constant irradiation conditions. A portion of each sample was dissolved in benzene-d₆ and a ³¹P{¹H} NMR spectrum was recorded to survey the result of the experiment.

5a. Complex **5a** (11 mg, 0.011 mmol) was irradiated with sunlight for approximately 12 days. Integration of the signals in the corresponding ³¹P{¹H} NMR spectrum revealed nearly 90% conversion of **5a** to **6a**.

δ_p (81 MHz, C₆D₆) 51.17 (s with ¹⁹⁵Pt satellites, ¹*J*_{Pt} = 3102 Hz, residual **5a**), 50.59 (d with ¹⁹⁵Pt satellites, ¹*J*_{Pt} = 2467 Hz, ²*J*_{PP} = 3.2 Hz, **6a**), 49.23 (d with ¹⁹⁵Pt satellites, ¹*J*_{Pt} = 1575 Hz, ²*J*_{PP} = 3.2 Hz, **6a**).

5b. Complex **5b** (16 mg, 0.016 mmol) was irradiated with sunlight for approximately 10 days. Integration of the signals in the corresponding ³¹P{¹H} NMR spectrum revealed 45% conversion of **5b** to **6b**.

δ_p (81 MHz, C₆D₆) 51.77 (s with ¹⁹⁵Pt satellites, ¹*J*_{Pt} = 3132 Hz, residual **5b**), 50.22 (d with ¹⁹⁵Pt satellites, ¹*J*_{Pt} = 2454 Hz, ²*J*_{PP} = 3.0 Hz, **6b**), 48.89 (d with ¹⁹⁵Pt satellites, ¹*J*_{Pt} = 1615 Hz, ²*J*_{PP} = 3.0 Hz, **6b**).

5c. Complex **5c** (13 mg, 0.015 mmol) was irradiated with sunlight for approximately 11 days. Integration of the signals in the corresponding ³¹P{¹H} NMR spectrum revealed 25% conversion of **5c** to **6c**.

δ_p (81 MHz, C₆D₆) 52.38 (s with ¹⁹⁵Pt satellites, ¹*J*_{Pt} = 3149 Hz, residual **5c**), 50.50 (d with ¹⁹⁵Pt satellites, ¹*J*_{Pt} = 2469 Hz, ²*J*_{PP} = 2.8 Hz, **6c**), 48.57 (d with ¹⁹⁵Pt satellites, ¹*J*_{Pt} = 1561 Hz, ²*J*_{PP} = 2.8 Hz, **6c**).

5d-g and 9b. The appropriate (diphosphine)(η²-tolane)Pt⁰ complex (12 mg, 0.012–0.015 mmol) was irradiated with sunlight for approximately 14 days. The corresponding ³¹P{¹H} NMR spectrum showed only the resonances of the starting material. No evidence for C–C bond activation was observed in any case.

9a. Orange crystals of **9a** (98 mg, 0.110 mmol) were placed in a sample vial and irradiated as described above for 50 days to ensure full conversion into **10a**. The reaction progress was checked

by ³¹P{¹H} NMR spectroscopy. After completion of the reaction **10a** was obtained as yellow powder (88 mg, 90%).

Mp: 175 °C (dec.); δ_H (400 MHz, CD₂Cl₂) 8.08 (d, ³*J*_{H,H} = 8.0 Hz, 2 H, *H*-4 and *H*-5 of dppn), 7.62–7.41 (m, 8 H, *H*-2, *H*-3, *H*-6 and *H*-7 of dppn), 7.37–7.16 (m, 10 H), 7.06 (m, 2 H), 7.01–6.79 (m, 6 H), 6.73 (m, 3 H), 6.60 (m, 2 H), 6.42 (m, 1 H), 2.40 (s, 3 H, CH₃), 1.88 (s, 3 H, CH₃); δ_c (100 MHz, CD₂Cl₂) 159.7 (m), 143.1 (m), 138.9 (s), 138.5 (s), 136.4 (m including 2 different C-atoms), 135.1 (s), 134.7 (m including 2 different C-atoms), 134.2 (m including 2 different C-atoms), 133.7 (m including 2 different C-atoms), 131.5 (s), 130.7 (s), 130.2 (s), 128.9 (m), 128.5 (m including 3 different C-atoms), 127.8 (m), 125.7 (m), 124.9 (m including 2 different C-atoms), 123.8 (m), 121.3 (s), 26.9 (s, CH₃), 20.1 (s, CH₃); δ_p (81 MHz, CD₂Cl₂) 11.92 (d with ¹⁹⁵Pt satellites, ¹*J*_{Pt} = 2427 Hz, ²*J*_{PP} = 34 Hz), 8.98 (d with ¹⁹⁵Pt satellites, ¹*J*_{Pt} = 1499 Hz, ²*J*_{PP} = 34 Hz); ν (KBr)/cm⁻¹ 3052 (s), 2982 (m), 2916 (m), 2112 (s, ν (C≡C)), 1595 (s), 1573 (m), 1480 (vs), 1435 (vs), 1329 (s), 1314 (s), 1185 (s), 1158 (s), 1096 (vs), 878 (m), 824 (s), 771 (vs), 743 (vs), 693 (vs), 585 (vs), 524 (vs), 499 (vs); *m/z*(DEI) 897 (10%, [M]⁺), 691 (20, [(dppn)Pt]⁺), 206 (100, [4c]⁺); Anal. calcd. for C₅₀H₄₀P₂Pt · 0.25 CH₂Cl₂: C 65.67, H 4.44; Found C 65.90, H 4.57.

Irradiation experiments in solution

The appropriate (diphosphine)(η²-tolane)Pt⁰ complex was dissolved in toluene and put in a round bottom flask. These solutions were irradiated with sunlight for the stated periods and the reaction progress was checked by TLC. After completion of the reactions the solvent was removed under reduced pressure and the residue was worked up by column chromatography to isolate the corresponding products. In the case of **5c**, **5g**, **5f** and **9a**, this work up procedure failed.

5a. A solution of **5a** (120 mg, 0.123 mmol) in toluene (60 mL) was irradiated with sunlight for approximately 30 days. After removing the solvent the residue was chromatographed on silica gel using dichloromethane–hexane (2/1) → dichloromethane as eluent to yield **6a** (45 mg, 37%) as pale yellow powder.

Mp: 158 °C (dec.); δ_H (400 MHz, CD₂Cl₂) 7.75 (m, 5 H), 7.67 (m, 1 H), 7.54–7.42 (m, 11 H), 7.34 (m, 8 H), 7.20 (m, 2 H), 7.05 (m, 1 H), 6.97 (m, 2 H), 6.81 (m, 2 H); δ_c (100 MHz, CD₂Cl₂) 155.2 (m), 139.8 (m), 134.4 (m), 134.1 (m, including 3 different C-atoms), 132.8 (s), 132.5 (m, including 2 different C-atoms), 131.9 (s), 131.2 (m, including 2 different C-atoms), 130.0 (m), 129.6 (s), 129.0 (m, including 2 different C-atoms), 119.0 (s), 116.8 (s); δ_p (81 MHz, CD₂Cl₂) 50.33 (d with ¹⁹⁵Pt satellites, ¹*J*_{Pt} = 2493 Hz, ²*J*_{PP} = 4.0 Hz), 49.01 (d with ¹⁹⁵Pt satellites, ¹*J*_{Pt} = 1603 Hz, ²*J*_{PP} = 4.0 Hz); ν (KBr)/cm⁻¹ 3054 (m), 2112 (s, ν (C≡C)), 1620 (w), 1581 (w), 1481 (vs), 1468 (s), 1435 (vs), 1210 (m), 1185 (m), 1114 (s), 1100 (vs), 1069 (s), 1003 (vs), 824 (s), 799 (s), 745 (s), 693 (vs), 670 (s), 551 (vs), 532 (vs), 506 (s); *m/z*(DEI) 977 (0.1%, [M]⁺), 897 (0.05, [M – Br]⁺), 721 (1, [(dppbe)PtBr]⁺); Anal. calcd. for C₄₄H₃₂Br₂P₂Pt: C 54.06, H 3.30, Br 16.35; Found C 54.27, H 3.38, Br 16.76.

5b. A solution of **5b** (237 mg, 0.236 mmol) in toluene (60 mL) was irradiated with sunlight for approximately 21 days. After removing the solvent the residue was chromatographed on silica gel using dichloromethane–hexane (2/1) → dichloromethane as

Table 2 Crystal data and refinement details for the X-ray structure determinations

Compound	5a	5b	5c	5d	5e	6b	7b	9a	9b
Formula	C ₄₄ H ₃₂ Br ₂ Pt	C ₄₆ H ₃₆ Br ₂ Pt	C ₄₆ H ₃₈ Pt	C ₄₃ H ₃₃ NPt	C ₄₂ H ₃₂ N ₂ Pt	C ₄₆ H ₃₆ Br ₂ Pt	C ₄₆ H ₃₆ Br ₂ Pt, C ₄ H ₈ O	C ₅₀ H ₄₀ Pt, C ₆ H ₆	C ₄₈ H ₄₂ Pt, C ₆ H ₆
Fw/g mol ⁻¹	977.55	1005.60	847.79	820.73	821.73	1005.60	1077.70	975.96	953.95
T/°C	-90(2)	-90(2)	-90(2)	-90(2)	-90(2)	-90(2)	-90(2)	-90(2)	-90(2)
Crystal system	Triclinic	Orthorhombic	Triclinic	Triclinic	Triclinic	Triclinic	Monoclinic	Triclinic	Triclinic
Space group	<i>P</i> $\bar{1}$	<i>Pbca</i>	<i>P</i> $\bar{1}$	<i>P</i> $\bar{1}$	<i>P</i> $\bar{1}$	<i>P</i> $\bar{1}$	<i>P</i> ₂ / <i>n</i>	<i>P</i> $\bar{1}$	<i>P</i> $\bar{1}$
<i>a</i> /Å	10.7128(4)	20.5293(3)	11.1682(5)	11.3596(4)	8.9010(4)	8.9257(2)	15.3444(5)	11.8366(5)	11.6006(5)
<i>b</i> /Å	11.4086(4)	16.4027(2)	12.2745(5)	11.5124(3)	11.0800(6)	11.2405(4)	15.6009(3)	12.6126(5)	12.9579(5)
<i>c</i> /Å	16.6238(6)	23.2611(3)	15.0911(7)	14.0287(5)	19.0760(7)	20.9629(8)	21.3260(6)	15.7836(9)	15.4685(5)
α (°)	100.791(2)	90	79.550(2)	71.401(2)	103.772(3)	78.7990(10)	90	102.484(2)	91.791(2)
β (°)	96.609(2)	90	69.759(2)	83.585(2)	96.509(2)	83.363(2)	111.085(2)	107.407(3)	107.389(2)
γ (°)	107.566(2)	90	69.043(2)	88.476(2)	107.308(2)	69.013(2)	90	95.895(3)	103.098(2)
<i>V</i> /Å ³	1870.52(12)	7832.85(18)	1808.67(14)	1727.8(1)	1709.75(14)	1923.84(11)	4763.4(2)	2159.55(18)	2148.93(14)
<i>Z</i>	2	8	2	2	2	2	4	2	2
ρ /g cm ⁻³	1.736	1.705	1.557	1.578	1.596	1.736	1.503	1.501	1.474
μ /cm ⁻¹	60.03	57.37	40	41.85	42.3	58.4	47.24	33.61	33.76
Measured data	11771	48171	12759	12393	12065	13479	31984	15004	15688
Data with									
<i>I</i> > 2 σ (<i>I</i>)	6807	6750	6772	6421	6139	6971	7025	7358	7398
Unique data/ <i>R</i> _{int}	7820/0.0485	8934/0.0822	8218/0.0447	7859/0.0494	7769/0.0502	8752/0.0332	10847/0.0669	9765/0.0365	9765/0.0470
<i>wR</i> ₂ (all data, on <i>F</i> ²) ^a	0.1268	0.0775	0.0902	0.0912	0.0996	0.0962	0.1483	0.1090	0.1226
<i>R</i> ₁ (<i>I</i> > 2 σ (<i>I</i>)) ^a	0.0482	0.0349	0.0451	0.0420	0.0470	0.0426	0.0534	0.0469	0.0526
<i>s</i> ^b	1.048	1.036	1.020	1.018	1.060	1.008	1.004	1.023	1.011
Res. dens./e Å ⁻³	1.396/-1.646	1.298/-1.458	1.471/-1.288	1.078/-1.469	1.094/-1.133	1.318/-1.457	1.476/-1.506	1.530/-1.432	1.657/-1.741
Absorpt. method	NONE	NONE	NONE	NONE	NONE	NONE	NONE	NONE	NONE
CCDC No.	743160	743161	743162	743163	743164	743165	743166	743167	743269

^a Definition of the *R* indices: $R_1 = (\sum ||F_o| - |F_c||) / \sum |F_o|$; $wR_2 = \{\sum [w(F_o^2 - F_c^2)^2] / \sum [w(F_o^2)^2]\}^{1/2}$ with $w^{-1} = \sigma^2(F_o^2) + (aP)^2 + bP$; $P = [2F_c^2 + \text{Max}(F_o^2)]/3$; ^b $s = \{\sum [w(F_o^2 - F_c^2)^2] / (N_o - N_p)\}^{1/2}$.

eluent to yield **6b** (60 mg, 25%) as white powder and **7b** (57 mg, 24%) as yellow crystals.

6b. Mp: >230 °C; δ_H (400 MHz, CD₂Cl₂) 7.84 (m, 2 H), 7.77 (m, 1 H), 7.66 (m, 5 H), 7.56–7.38 (m, 12 H), 7.24 (m, 2 H), 7.12 (s, 1 H), 7.02 (dd, ³*J*_{H,H} = 8.2 Hz, ⁴*J*_{H,H} = 1.9 Hz, 1 H), 6.92 (m, 4 H), 6.83 (m, 1 H), 6.73 (m, 1 H), 1.94 (s, 3 H, CH₃), 1.93 (s, 3 H, CH₃); δ_C (100 MHz, CD₂Cl₂) 147.3 (m), 141.8 (m), 138.3 (m), 134.4 (m, including 3 different C-atoms), 133.8 (m), 132.7 (m, including 3 different C-atoms), 131.8 (m, including 2 different C-atoms), 131.1 (m), 129.1 (m, including 2 different C-atoms), 128.7 (m), 128.2 (s), 126.5 (m), 118.4 (s), 116.9 (s), 25.9 (s, CH₃), 20.6 (s, CH₃); δ_P (81 MHz, CD₂Cl₂) 50.08 (d with ¹⁹⁵Pt satellites, ¹*J*_{Pt} = 2474 Hz, ²*J*_{Pt} = 4.0 Hz), 48.86 (d with ¹⁹⁵Pt satellites, ¹*J*_{Pt} = 1639 Hz, ²*J*_{Pt} = 4.0 Hz); ν (KBr)/cm⁻¹ 3053 (s), 2950 (w), 2110 (s, ν (C≡C)), 1619 (m), 1472 (vs), 1435 (vs), 1187 (s), 1100 (vs), 1028 (s), 865 (m), 839 (m), 815 (m), 745 (s), 693 (vs), 670 (s), 552 (vs), 532 (vs), 506 (vs); *m/z*(DEI) 1006 (2%, [M]⁺), 924 (4, [M – Br]⁺), 721 (35, [(dppbe)PtBr]⁺), 641 (12, [(dppbe)Pt]⁺), 487 (4, [(dppbe)Pt – 2×Ph]⁺), 364 (4, [4b]⁺); Anal. calcd. for C₄₆H₃₆Br₂Pt: C 54.94, H 3.61, Br 15.89; Found C 55.28, H 3.59, Br 15.31.

7b. Mp: 151 °C (dec.); δ_H (400 MHz, CD₂Cl₂) 7.76 (m, 4 H), 7.63 (m, 1 H), 7.51 (m, 11 H), 7.38 (m, 10 H), 7.29 (m, 2 H), 6.98 (m, 2 H), 6.80 (d, ³*J*_{H,H} = 7.0 Hz, 1 H), 2.45 (s, 3 H, CH₃), 2.13 (s, 3 H, CH₃); δ_C (100 MHz, CD₂Cl₂) 136.5 (m), 142.2 (m), 139.0 (m), 138.1 (m), 135.4 (m), 134.0 (m, including 5 different C-atoms), 133.1 (s), 132.6 (m), 131.6 (m), 131.3 (s), 130.1 (m), 128.9 (m, including 3 different C-atoms), 123.6 (s), 121.5 (s), 117.0 (m), 95.6 (s, C≡C), 89.5 (s, C≡C), 21.0 (s, CH₃), 20.7 (s, CH₃); δ_P (81 MHz, CD₂Cl₂) 49.64 (d with ¹⁹⁵Pt satellites, ¹*J*_{Pt} = 1684 Hz, ²*J*_{Pt} = 3.5 Hz), 43.01

(d with ¹⁹⁵Pt satellites, ¹*J*_{Pt} = 4090 Hz, ²*J*_{Pt} = 3.5 Hz); ν (KBr)/cm⁻¹ 3053 (m), 2973 (m), 2868 (m), 2205 (m, ν (C≡C)), 1631 (m), 1573 (s), 1484 (vs), 1435 (vs), 1190 (s), 1100 (vs), 881 (s), 816 (s), 746 (s), 693 (vs), 671 (s), 560 (vs), 533 (vs), 505 (vs); *m/z*(DEI) 1006 (2%, [M]⁺), 924 (3, [M – Br]⁺), 721 (40, [(dppbe)PtBr]⁺), 641 (10, [(dppbe)Pt]⁺), 283 (80, [4b – Br]⁺); Anal. calcd for C₄₆H₃₆Br₂Pt · 2 C₄H₈O: C 56.41, H 4.56, Br 13.90; Found C 56.84, H 4.49, Br 14.03.

Crystal structure determinations

The intensity data for the compounds were collected on a Nonius KappaCCD diffractometer using graphite-monochromated Mo-K α radiation. Data were corrected for Lorentz and polarization effects but not for absorption effects.^{32,33} The structures were solved by direct methods (SHELXS)³⁴ and refined by full-matrix least squares techniques against *F*_o² (SHELXL-97) (Table 2).³⁵ All hydrogen atoms were included at calculated positions with fixed thermal parameters. All non-disordered non-hydrogen atoms were refined anisotropically.³⁵ Diamond 3.0b as well as POV-Ray 3.6.1c were used for structure representations. CCDC-743160 (for **5a**), -743161 (for **5b**), -743162 (for **5c**), -743163 (for **5d**), -743164 (for **5e**), -743165 (for **6b**), -743166 (for **7b**), -743167 (for **9a**) and -743269 (for **9b**) contain the supplementary crystallographic data for this paper.† These data can be obtained free of charge from the Cambridge Crystallographic Centre via www.ccdc.cam.ac.uk/data_request/cif.

Computational details

See part B.†

Acknowledgements

The donation of K_2PtCl_4 by the Heraeus GmbH is gratefully acknowledged by the authors. Additionally, we thank the students A. Pospiech and M. Assmann for preparing the phosphane ligands as well as some tolanes. Financial support from the Carl-Zeiss Stiftung (D.E.) is also acknowledged. Finally, we thank the reviewers for their valuable comments and suggestions.

Notes and references

- M. Murakami and Y. Ito, in *Topics in Organometallic Chemistry*, ed. S. Murai, Springer, Berlin, 1999, vol. 3, pp. 97–129; K. C. Bishop III, *Chem. Rev.*, 1976, **76**, 461–486.
- P. W. Jennings and L. L. Johnson, *Chem. Rev.*, 1994, **94**, 2241–2290; R. H. Crabtree, *Chem. Rev.*, 1985, **85**, 245–269.
- B. Rytbchinski and D. Milstein, *Angew. Chem., Int. Ed.*, 1999, **38**, 870–883.
- C. Perthuisot and W. D. Jones, *J. Am. Chem. Soc.*, 1994, **116**, 3647–3648; C. Perthuisot, B. L. Edelbach, D. L. Zubris and W. D. Jones, *Organometallics*, 1997, **16**, 2016–2023; B. L. Edelbach, R. J. Lachicotte and W. D. Jones, *J. Am. Chem. Soc.*, 1998, **120**, 2843–2853; W. D. Jones, *Nature*, 1993, **364**, 676–677; D. D. Wick, T. O. Northcutt, R. J. Lachicotte and W. D. Jones, *Organometallics*, 1998, **17**, 4484–4492; T. Nishimura and K. Ohe, *J. Am. Chem. Soc.*, 1999, **121**, 2645–2646; T. Nishimura and S. Uemura, *J. Am. Chem. Soc.*, 1999, **121**, 11010–11011; Z. Lu, C.-H. Jun, S. R. de Gala, O. Eisenstein and R. H. Crabtree, *Organometallics*, 1995, **14**, 1168–1175; Z. Lu, C.-H. Jun, S. R. de Gala, M. Sigalas, O. Eisenstein and R. H. Crabtree, *J. Chem. Soc., Chem. Commun.*, 1993, 1877–1880; H. Schwager, S. Spyroudis and K. P. C. Vollhardt, *J. Organomet. Chem.*, 1990, **382**, 191–200; J. J. Eisch, A. M. Piotrowski, K. I. Han, C. Krüger and Y. H. Tsay, *Organometallics*, 1985, **4**, 224–231; T. C. Flood and J. A. Statler, *Organometallics*, 1984, **3**, 1795–1803.
- M. Gozin, A. Weisman, Y. Ben-David and D. Milstein, *Nature*, 1993, **364**, 699–701; M. Gozin, M. Aizenberg, S.-Y. Liou, A. Weisman, Y. Ben-David and D. Milstein, *Nature*, 1994, **370**, 42–44; R. H. Crabtree, R. P. Dion, D. J. Gibboni, D. V. McGrath and E. M. Holt, *J. Am. Chem. Soc.*, 1986, **108**, 7222–7227; A. Barretta, F. G. N. Cloke, A. Feigenbaum, M. L. H. Green, A. Gourdon and K. Prout, *J. Chem. Soc., Chem. Commun.*, 1981, 156–158; M. Gandelman, A. Vigalok, L. J. W. Shimon and D. Milstein, *Organometallics*, 1997, **16**, 3981–3986; S.-Y. Liou, M. Gozin and D. Milstein, *J. Am. Chem. Soc.*, 1995, **117**, 9774–9775; S.-Y. Liou, M. Gozin and D. Milstein, *J. Chem. Soc., Chem. Commun.*, 1995, 1965–1966.
- B. Rytbchinski, A. Vigalok, Y. Ben-David and D. Milstein, *J. Am. Chem. Soc.*, 1996, **118**, 12406–12415; M. E. van der Boom, H.-B. Kraatz, Y. Ben-David and D. Milstein, *Chem. Commun.*, 1996, 2167–2168.
- R. H. Crabtree and R. P. Dion, *J. Chem. Soc., Chem. Commun.*, 1984, 1260–1261; J. J. Garcia and W. D. Jones, *Organometallics*, 2000, **19**, 5544–5545; J. W. Suggs and S. D. Cox, *J. Organomet. Chem.*, 1981, **221**, 199–201; C.-H. Jun, C. W. Moon, H. Lee and D.-Y. Lee, *J. Mol. Catal. A: Chem.*, 2002, **189**, 145–156.
- J. J. Low and W. A. Goddard III, *J. Am. Chem. Soc.*, 1984, **106**, 8321–8322; P. E. M. Siegbahn and M. R. A. Blomberg, *J. Am. Chem. Soc.*, 1992, **114**, 10548–10556.
- J. A. Martinho, Simões and J. A. Beauchamp, *Chem. Rev.*, 1990, **90**, 629–688.
- S. P. Nolan, C. D. Hoff, P. O. Stoutland, L. J. Newman, J. M. Buchanan, R. G. Bergman, G. K. Young and K. S. Peters, *J. Am. Chem. Soc.*, 1987, **109**, 3143–3145; W. D. Jones and F. J. Feher, *J. Am. Chem. Soc.*, 1984, **106**, 1650–1663; P. O. Stoutland, R. G. Bergman, S. P. Nolan and C. D. Hoff, *Polyhedron*, 1988, **7**, 1429–1440.
- C. Müller, C. N. Iverson, R. J. Lachicotte and W. D. Jones, *J. Am. Chem. Soc.*, 2001, **123**, 9718–9719; A. Gunay, C. Müller, R. J. Lachicotte, W. W. Brennessel and W. D. Jones, *Organometallics*, 2009, **28**, 6524–6530.
- A. Gunay and W. D. Jones, *J. Am. Chem. Soc.*, 2007, **129**, 8729–8735.
- H. Petzold, T. Weisheit, H. Görls, H. Breitzke, G. Buntkowsky, D. Escudero, L. González and W. Weigand, *Dalton Trans.*, 2008, 1979–1981.
- H. Petzold, H. Görls and W. Weigand, *J. Organomet. Chem.*, 2007, **692**, 2736–2742.
- K. Zhang, J. Hu, K. C. Chan, K. Y. Wong and J. H. K. Yip, *Eur. J. Inorg. Chem.*, 2007, 384–393.
- A. Fürstner and P. W. Davies, *Angew. Chem.*, 2007, **119**, 3478–3519; A. Fürstner and P. W. Davies, *Angew. Chem., Int. Ed.*, 2007, **46**, 3410–3449.
- D. Escudero, M. Assmann, A. Pospiech, W. Weigand and L. González, *Chem. Phys. Phys. Chem.*, 2009, **11**, 4593–4600.
- K. Tanaka and F. Toda, *Chem. Rev.*, 2000, **100**, 1025–1074 and references therein.
- O. V. Zenkina, A. Karton, D. Freeman, L. J. W. Shimon, J. M. L. Martin and M. E. van der Boom, *Inorg. Chem.*, 2008, **47**, 5114–5121.
- O. Zenkina, M. Altman, G. Leitus, L. J. W. Shimon, R. Cohen and M. E. van der Boom, *Organometallics*, 2007, **26**, 4528–4534; D. Strawser, A. Karton, O. V. Zenkina, M. A. Iron, L. J. W. Shimon, J. M. L. Martin and M. E. van der Boom, *J. Am. Chem. Soc.*, 2005, **127**, 9322–9323; A. C. B. Lucassen, L. J. W. Shimon and M. E. van der Boom, *Organometallics*, 2006, **25**, 3308–3310.
- T. Weisheit, H. Petzold, H. Görls, G. Mloston and W. Weigand, *Eur. J. Inorg. Chem.*, 2009, 3545–3551.
- T. Niksch, H. Görls, M. Friedrich, R. Oilunkaniemi, R. Laitinen and W. Weigand, *Eur. J. Inorg. Chem.*, 2009, 74–94.
- P. Hofmann, H. Heiß and G. Müller, *Z. Naturforsch.*, 1987, **42b**, 395–409; C. Massera and G. Frenking, *Organometallics*, 2003, **22**, 2758–2765.
- I. M. Al-Najjar, *Inorg. Chim. Acta*, 1987, **128**, 93–104.
- J.-E. Song, B.-O. Kim and Y. Ha, *Mater. Sci. Eng., C*, 2004, **24**, 191–194.
- M. Camalli, F. Caruso, S. Chaloupka, E. M. Leber, H. Rimml and L. M. Venanzi, *Helv. Chim. Acta*, 1990, **73**, 2263–2274.
- J. Okubo, H. Shinozaki, T. Koitabashi and R. Yomura, *Bull. Chem. Soc. Jpn.*, 1998, **71**, 329–335.
- M. J. Mio, L. C. Kopel, J. B. Braun, T. L. Gadzikwa, K. L. Hull, R. G. Brisbois, C. J. Markworth and P. A. Criecco, *Org. Lett.*, 2002, **4**, 3199–3202.
- V. Mouriès, R. Waschbüsch, J. Carran and P. Savignac, *Synthesis*, 1998, 271–274.
- M.-J. Wu, L.-M. Wei, C.-F. Lin, S.-P. Leou and L.-L. Wei, *Tetrahedron*, 2001, **57**, 7839–7844.
- C. Y. Ju, Y. Chong, J. F. Kayyem and M. Gozin, *J. Org. Chem.*, 1999, **64**, 2070–2079.
- COLLECT, Data Collection Software; Nonius B.V., Netherlands, 1998.
- Z. Otwinowski and W. Minor, “Processing of X-Ray Diffraction Data Collected in Oscillation Mode” in *Methods in Enzymology: Macromolecular Crystallography, Part A*, ed. C. W. Carter, and R. M. Sweet, Academic Press, San Diego, 1997, Vol. 276, pp. 307–326.
- G. M. Sheldrick, *Acta Crystallogr., Sect. A: Found. Crystallogr.*, 1990, **46**, 467–473.
- G. M. Sheldrick *SHELXL-97* (Release 97-2), University of Göttingen, Germany, 1997.